



**University of Dundee**

**Rapid and scale-independent microfluidic manufacture of liposomes entrapping protein incorporating in-line purification and at-line size monitoring**

Forbes, Neil; Hussain, Maryam T.; Briuglia, Maria L.; Edwards, Darren Y.; Horst, Joop H. Ter; Szita, Nicolas

*Published in:*  
International Journal of Pharmaceutics

*DOI:*  
[10.1016/j.ijpharm.2018.11.060](https://doi.org/10.1016/j.ijpharm.2018.11.060)

*Publication date:*  
2019

*Licence:*  
CC BY-NC-ND

*Document Version*  
Peer reviewed version

[Link to publication in Discovery Research Portal](#)

*Citation for published version (APA):*

Forbes, N., Hussain, M. T., Briuglia, M. L., Edwards, D. Y., Horst, J. H. T., Szita, N., & Perrie, Y. (2019). Rapid and scale-independent microfluidic manufacture of liposomes entrapping protein incorporating in-line purification and at-line size monitoring. *International Journal of Pharmaceutics*, 556, 68-81.  
<https://doi.org/10.1016/j.ijpharm.2018.11.060>

**General rights**

Copyright and moral rights for the publications made accessible in Discovery Research Portal are retained by the authors and/or other copyright owners and it is a condition of accessing publications that users recognise and abide by the legal requirements associated with these rights.

**Take down policy**

If you believe that this document breaches copyright please contact us providing details, and we will remove access to the work immediately and investigate your claim.

1 Title: Rapid and scale-independent microfluidic manufacture of liposomes entrapping protein  
2 incorporating in-line purification and at-line size monitoring.

3 Authors: Neil Forbes<sup>1+</sup>, Maryam T. Hussain<sup>1+</sup>, Maria L. Briuglia<sup>2</sup>, Darren Y Edwards<sup>3</sup>, Joop H.  
4 ter Horst<sup>2</sup>, Nicolas Szita<sup>4</sup> and Yvonne Perrie <sup>1\*</sup>

5 <sup>1</sup>Strathclyde Institute of Pharmacy and Biomedical Sciences, University of Strathclyde,  
6 Glasgow, United Kingdom.

7 <sup>2</sup>EPSRC Centre for Innovative Manufacturing in Continuous Manufacturing and Crystallisation,  
8 University of Strathclyde, Glasgow, United Kingdom.

9 <sup>3</sup>University of Dundee, Nethergate, Dundee, Scotland, UK, DD1 4HN

10 <sup>4</sup>Department of Biochemical Engineering, University College London, London, WC1H 0AH,  
11 United Kingdom.

12 \*these authors contributed equally to this work.

13 **Key Words:** Liposomes, protein, microfluidics, manufacture, continuous, scale-independent,  
14 formulation.

15

16 **Corresponding author:**

17 Professor Yvonne Perrie

18 Strathclyde Institute of Pharmacy and Biomedical Sciences,

19 161 Cathedral St,

20 University of Strathclyde,

21 Glasgow, G4 0RE

22 Scotland.

23 [yvonne.perrie@strath.ac.uk](mailto:yvonne.perrie@strath.ac.uk)

24

25

26 **Abstract**

27 Within this paper we present work that has the ability to de-risk the translation of liposomes from  
28 bench to the clinic. We have used microfluidics for the rapid and scale-independent manufacture of  
29 liposomes and have incorporated in-line purification and at-line monitoring of particle size. Using this  
30 process, we have manufactured a range of neutral and anionic liposomes incorporating protein.  
31 Factors investigated include the microfluidics operating parameters (flow rate ratio (FRR) and total  
32 flow rate (TFR)) and the liposome formulation. From these studies, we demonstrate that FRR is a key  
33 factor influencing liposome size, protein loading and release profiles. The liposome formulations  
34 produced by microfluidics offer high protein loading (20-35 %) compared to production by sonication  
35 or extrusion (< 5%). This high loading achieved by microfluidics results from the manufacturing process  
36 and is independent of lipid selection and concentration across the range tested. Using in-line  
37 purification and at-line size monitoring, we outline the normal operating range for effective  
38 production of size controlled (60 to 100 nm), homogenous (PDI <0.2) high load liposomes. This easy  
39 microfluidic process provides a translational manufacturing pathway for liposomes in a wide-range of  
40 applications.

## 41 **1. Introduction**

42 Protein-based therapies are a key tool in healthcare with approximately 240 FDA approved protein  
43 and peptides available (Fosgerau and Hoffmann, 2015; Lu et al., 2014; Usmani et al., 2017). These  
44 proteins and peptides can be used for the treatment and amelioration of a range of diseases as well  
45 as used for diagnostic purposes and vaccines (Carter, 2011). However, there are still a number of  
46 associated challenges with the delivery of proteins including their sensitivity to both chemical and  
47 physical degradation which can result in low bioavailability and short half-life after in vivo  
48 administration (Lee and Yuk, 2007). To address this, a wide range of drug delivery systems have been  
49 investigated including liposomes. Liposomes can offer targeting, protection to their payload, high  
50 biocompatibility and low toxicity (Torchilin and Lukyanov, 2003) and there are a notable number of  
51 liposomal formulations on the market or undergoing trials, including a range of anticancer agents,  
52 antifungal systems and vaccines such as Inflexal V – a virosome-based vaccine formulation for  
53 influenza (Bulbake et al., 2017).

54 However, the manufacture and production of liposomes is challenging, particularly when considering  
55 the entrapment of proteins. Manufacturing conditions including temperature, high pressure, non-  
56 aqueous solvents, metal ions, detergents, incompatible pH and/or ionic strength, and shearing can all  
57 impact on the chemical and physical stability of proteins. Furthermore, many of the methods adopted  
58 give poor encapsulation efficiency, as summarised in Table 1. Although methods such as reverse phase  
59 evaporation have been developed to combat some of these issues, this process offers limited size  
60 control and produces formulations that are very heterogeneous (Szoka and Papahadjopoulos, 1978).  
61 In addition to this, the liposome formulation can also influence protein encapsulation with factors  
62 such as the lipid(s) used, the amount of cholesterol and protein concentration all shown to effect the  
63 amount of protein encapsulation (Xu et al., 2012).

64 Microfluidics is an alternative technology that can be used to produce liposomes. It uses a lab-on-a-  
65 chip approach and can be defined as the manipulation of small volumes in a controlled microchannel  
66 environment, which encourages mixing (Whitesides, 2006). Microfluidics, unlike the thin film lipid  
67 hydration method, produces liposomes using a 'bottom-up' approach (Akbarzadeh et al., 2013). In  
68 contrast to 'top-down' methods which rely on size reduction of larger multilamellar vesicles,  
69 microfluidics results in the formation of small liposomes from individual lipid monomers and thus no  
70 additional size reduction method is needed. Microfluidics offers both ease of scale-up and use for high  
71 throughput screening as it can also run with small quantities, whilst maintaining high resolution and  
72 sensitivity. This, along with the fact it can decrease production cost and time has led to microfluidics  
73 becoming increasingly popular in the pharmaceutical industry.

74 In microfluidics cartridges, fluid flows through micro-channels that converge; the organic phase (lipids  
75 dissolved in alcohol) flows through one channel whilst the aqueous phase (buffer) flows through the  
76 other. From the point the two fluid streams converge formation of liposomes begins to occur at the  
77 liquid interface. The mixing of the organic phase with the aqueous phase causes a decrease in the  
78 concentration of alcohol, due to diffusion (Capretto et al., 2013). As such, the low concentration of  
79 alcohol causes an increase in polarity and the lipids to precipitate, resulting in the self-assembly of  
80 vesicles with a lipid bilayer and an aqueous core (Jahn et al., 2010; Zook and Vreeland, 2010). Assembly  
81 can be controlled by varying the speed (known as the Total Flow Rate (TFR)) and mixing ratio (referred  
82 to as the Flow Rate Ratio) of the fluid flows through the channels (Jahn et al., 2007). Recently, several  
83 studies have shown the potential of microfluidics to produce liposomes in a range of sizes, as well as  
84 encapsulate different materials including small interfering RNA (Belliveau et al., 2012; Chen et al.,  
85 2012), low solubility drugs (Kastner et al., 2015), and combinations of aqueous and bilayer drug loaded  
86 liposomes (Joshi et al., 2016). Furthermore, Dimov et al (Dimov et al., 2017), demonstrated a lab-on-  
87 bench scale set-up for the manufacture of liposomes in a scale independent manner using novel  
88 engineered equipment. Nonetheless, whilst research has shown the ability to encapsulate a range of  
89 biologics, the ability to scale up this process has not been systematically explored. Therefore, within  
90 this paper we investigate and demonstrate the use of microfluidics to encapsulate proteins in a scale-  
91 independent manner and we incorporate in-line purification and at-line particle size monitoring for  
92 in-process control and as a product validation tool.

## 93 **2. Materials and Methods.**

### 94 **2.1 Materials**

95 The lipids egg phosphatidylcholine (PC), 1,2-dimyristoyl-sn-glycero-3-phosphocholine (DMPC), 1,2-  
96 dipalmitoyl-sn-glycero-3-phosphocholine (DPPC), 1,2-distearoyl-sn-glycero-3-phosphocholine (DSPC),  
97 and L- $\alpha$ -phosphatidylserine (Brain PS, Porcine) were all purchased from Avanti Polar Lipids Inc.,  
98 Alabaster, AL, US. Cholesterol (cholesterol), Insulin, Ovalbumin (OVA), bovine serum albumin (BSA),  
99 Sucrose, trifluoroacetic acid and D9777-100ft dialysis tubing cellulose were purchased from Sigma  
100 Aldrich Company Ltd., Poole, UK. For ovalbumin purification by Tangential flow filtration (TFF), a  
101 modified polyethersulfone (mPES) 750 kD MWCO hollow fibre column was used (Spectrum Inc., Breda,  
102 The Netherlands). For release studies, Biotech CE Tubing MWCO 300 kD was used (Spectrum Inc.,  
103 Breda, The Netherlands). A Jupiter column (C18 (300 Å), 5  $\mu$ m, dimensions 4.60 X 150 mm) and a Luna  
104 column (C18(2), 5  $\mu$ m, dimensions 4.60 X 150 mm, pore size 100 Å) was used in HPLC and purchased  
105 from Phenomenex., Macclesfield, UK. The Pierce™ BCA Protein Assay kit, Dil Stain (1,1'-Dioctadecyl-  
106 3,3,3',3'- Tetramethylindocarbocyanine Perchlorate ('Dil'; DiIC18 (3)), HPLC grade methanol and 2-

107 propanol were purchased from Fisher Scientific, Loughborough, England, UK. All water and solvents  
108 used were HPLC grade.

## 109 **2.2. Liposome production**

### 110 **2.2.1 Liposomes prepared by extrusion and sonication**

111 Lipids were dissolved at required concentrations in a chloroform:methanol mixture (v/v 9:1) and  
112 placed under vacuum via rotatory evaporation for 6 minutes at 200 rpm in a heated (37°C) water bath  
113 to remove solvent. Hydration of the lipid film and protein encapsulation was achieved by the addition  
114 of phosphate buffered saline (PBS) (pH 7.3 ± 0.2) containing ovalbumin (0.25 mg/mL) at temperatures  
115 above the appropriate lipid transition temperature. Hand held extrusion was conducted on  
116 multilamellar vesicles (MLV) using a Mini Extruder from Avanti Polar Lipids Inc., Alabaster, AL, US.  
117 Liposomes (1 mg/mL) were extruded through incrementally decreasing pore sized membranes (0.5 –  
118 0.2 µm), with each sample being cycled through ten times. During extrusion, liposomes were held  
119 above their appropriate transition temperature. Size reduction of multilamellar vesicles was also  
120 achieved via sonication using a 9.5 mm titanium probe sonicator (Soniprep 150, MSE labs, UK) for 4  
121 minutes at 10 Hz. Again during this process, liposomes were held above their appropriate transition  
122 temperature.

### 123 **2.2.2. Liposomes prepared by microfluidics**

124 The preparation of liposomes by microfluidics was conducted on the Nanoasemblr® Benchtop system  
125 from Precision Nanosystems. Selected lipids were dissolved in methanol at specific concentrations  
126 (ranging primarily between 0.3 – 10 mg/mL total lipid) and injected through one of the two inlets on  
127 the microfluidics herringbone micromixer chip, whilst the aqueous phase (PBS; pH 7.3 ± 0.2) is injected  
128 into the second inlet. A number of production parameters can be controlled using the Nanoasemblr®  
129 software including the flow rate ratio (the ratio between the aqueous phase and the lipid phase) and  
130 the total flow rate (the speed at which the two inlets are injected through the chip). Flow rate ratios  
131 of 1:1, 3:1 and 5:1 were selected for testing as well as total flow rate speeds between 5 - 20 mL/min.  
132 For the production of protein loaded liposomes, ovalbumin was added to the aqueous phase at  
133 specific concentrations and the same principles for the production of empty liposomes was followed.  
134 Larger scale production of OVA loaded liposomes was prepared using the Nanoasemblr® Blaze™ (10  
135 mL to 1L) utilising the same production parameters as previously optimised on the Benchtop system  
136 (3:1 FRR, 15 mL/min), without the addition of a dilution factor.

137

138

### 139 **2.3. Quantification of lipid and liposome recovery**

140 HPLC- ELSD (high performance liquid chromatography- evaporative light scattering detector) was used  
141 to quantify the lipid recovery within liposomes. A Luna column (C18(2), 5  $\mu\text{m}$ , dimensions 4.60 X 150  
142 mm, pore size 100  $\text{\AA}$ ) was used to detect the lipids, at a flow rate of 2 mL/min. A twenty minute elution  
143 gradient, composed of solvent A (0.1% TFA in water) and solvent B (100% methanol) was used. During  
144 the first six minutes the gradient was 15:85 (A:B), at 6.1 minutes 0:100 (A:B) and then back to the  
145 initial gradient of 15:85 (A:B) from 15.1 to 20 minutes. The lipid recovery was calculated as a  
146 percentage in comparison to the initial concentration of the stock solution. Liposome recovery was  
147 calculated by incorporating the hydrophobic dye Dil Stain (1,1'-Dioctadecyl-3,3',3',3'-  
148 Tetramethylindocarbocyanine Perchlorate ('Dil'; DiIC18 (3)) (DiIC) at 0.2 mol% into the bilayer of the  
149 liposomes. Post production and during purification, aliquots of permeate was collected during the TFF  
150 process.

### 151 **2.4 Liposome purification via tangential flow filtration**

152 Liposome samples were purified using Krosflo Research lli tangential flow filtration system fitted with  
153 an mPES (modified polyethersulfone) column with a pore size of 750 kD. For removal of solvent and  
154 unentrapped protein, liposomal samples were circulated through the column and purified through  
155 difiltration, with fresh PBS being added at the same rate as the permeate leaving the column.

### 156 **2.5. Liposome characterisation**

157 Dynamic light scattering (DLS) was used to analyse the intensity mean diameter (z-average) and  
158 polydispersity index (PDI) of the liposomal formulations using a Malvern Zetasizer Nano-ZS (Malvern  
159 Instruments, Worcs., UK). All measurements were undertaken in triplicate. All readings were between  
160 6-9 attenuation and samples were diluted 1/10 with appropriate buffer. To continuously monitor  
161 particle size in an at-line process, the Zetasizer AT (Malvern Panlaytical Ltd, Malvern, UK) was used.  
162 The Zetasizer AT measured liposome size and PDI at a 1:10 dilution (liposomes to buffer). A buffer flow  
163 rate of 5 mL/min and liposome formulation flow rate of 0.5 mL/min were used. A total of 1 mL was  
164 required for each size measurement.

### 165 **2.6. Liposome morphology**

166 Images were taken on a Jeol 2011 with a 200kv beam using minimal dose protocol, scanned at low  
167 magnification and jumped to high magnification without exposing the sample to the beam first. The  
168 camera used was a Gatan ultrascan (2k by 2k pixels). Grids were lacey carbon, 200 mesh and were  
169 prepared by adding 8 microlitres of sample to a glow discharged grid, blotting from both sides for

170 approximately 5 seconds then plunging into nitrogen cooled ethane propane mix (70% ethane).  
171 CryoTEM pictures were taken at Warwick University, UK by Dr Saskia Bakker, Advanced Bioimaging  
172 Platform, and University of Warwick. Evaluation was performed at 15000x magnification.

## 173 **2.7. Encapsulated protein quantification**

174 Solubilisation of the liposomes to release entrapped protein was achieved following a previously  
175 published protocol (Fatouros and Antimisiaris, 2002) and modified for protein formulations. Briefly,  
176 liposomal samples were added at a 50/50 v/v ratio with solubilisation mixture (PBS / 2-Propanol 50/50  
177 v/v) and vortexed. Protein quantification was then determined using either UV-HPLC or BCA protein  
178 assay. For UV-HPLC, an Agilent 1100 Series HPLC (California, USA) was used to quantify the amount  
179 of OVA entrapped inside liposomes. All samples were run at 280 nm, using a C18 column (i.d. 150 X  
180 4.6 mm) from Phenomenex (Macclesfield, UK). A 1 mL/min flow rate was used with a twenty minute  
181 elution gradient, composed of solvent A (0.1% TFA in water) and solvent B (100% methanol). During  
182 the first ten minutes the gradient was 100: 0 (A: B), at 10.1 minutes 0: 100 (A: B) and then back to the  
183 initial gradient of 100: 0 (A: B) from 15.1 to 20 minutes. The injection volume for the sample is 20  $\mu$ L.  
184 For protein release studies, HPLC was used in conjunction with a SEDEX 90LT evaporative light  
185 scattering detector (ELSD) (Sedex sedere, Alfortville, France) to quantify the amount of OVA. A Jupiter  
186 A100 column was used to detect the OVA protein. The flow rate used was 1 mL/ min, with a gain of 8  
187 and an OVA peak appearing at 11.8 minutes. A standard calibration curve for OVA was established  
188 using various concentrations; the amount of encapsulated protein in liposomes produced by  
189 microfluidics and sonication was calculated using the peak area of the sample in relation to the  
190 standards. Protein quantification using BCA/ Micro BCA protein assay was carried out as per  
191 manufacturer's instructions. Briefly, samples were incubated with appropriate volume of working  
192 reagent and incubated at 37°C and the absorbance measured at 562 nm. Calibration curves were  
193 subjected to the inclusion of empty liposomes and solubilisation mixture and appropriate blanks were  
194 measured for subtraction of absorbance values.

## 195 **2.8 Circular dichroism**

196 The OVA protein integrity was tested after microfluidics and TFF. Untreated OVA (0.3 mg/ mL) in PBS  
197 was used as a control to test OVA integrity inside DSPC:Chol liposomes. The liposomes were made  
198 using 8 mg/mL initial lipid and 8 mg/ mL initial OVA at a 3:1 FRR and 15 mL/min TFR. The Chiroscan™-  
199 plus was used to analyse OVA using 20  $\mu$ L of the respective samples. The sample was placed in  
200 between two microscope slides and placed into a Suprasil® quartz absorption cuvette (Hellma,

201 Germany: path length of 1 mm). The measurement temperature was 25 °C and spectra recorded from  
202 180-260 nm range.

## 203 **2.9 Protein release studies**

204 Ovalbumin loaded liposomes (PC:Chol, DMPC:Chol, DPPC:Chol and DSPC:Chol) were produced using  
205 microfluidics using a 3:1 FRR and 15 mL/min TFR (4 mg/mL initial lipid and 0.25 mg/mL Ovalbumin).  
206 The DMPC:Chol formulation was selected, and made at both a 3:1 and 5:1 FRR (the TFR used was 15  
207 mL/min). The untrapped OVA and solvent was removed by TFF (12 mL wash cycle needed per mL  
208 of formulation). Purified formulations are used to investigate the rate of OVA release; 1 mL of the  
209 formulation was placed in a 300 kD dialysis bag in the presence of 25 mL of phosphate buffered saline  
210 (pH 7.3 ± 0.2). The samples were left for 0.5, 1, 3, 6, 18, 24, 48, 72, 96 and 120 hours at 37°C with  
211 agitation, after the allocated time the liposome formulation was collected and analysed by HPLC.

## 212 **2.10 Headspace Gas Chromatography**

213 Headspace gas chromatography (Agilent 7697A, Agilent Technologies, USA) was used to measure  
214 residual solvent content for liposomes produced by microfluidics and purified by tangential flow  
215 filtration. Solvent was measured using in an isothermal process using an Agilent 122-1334 column  
216 (30m x 250µm x 1.4 µm). The sample was held at 60°C for a minute before the temperature was  
217 ramped up to 80°C for 6 minutes.

## 218 **2.11 Statistical analysis**

219 Results are represented as mean ± SD with n = 3 independent batches. ANOVA tests were used to  
220 assess statistical significance, with a Tukey's post adhoc test (p value of less than 0.05). Where  
221 appropriate the similarity or differences between drug release profiles from various formulations was  
222 assessed by the  $f_2$  similarity test.

## 223 **3. Results and Discussion**

### 224 **3.1 Rapid and scalable manufacture of liposomes prepared by microfluidics: identifying the normal** 225 **operating range.**

226 We have previously reported on the use of microfluidics to manufacture liposomes entrapping DNA  
227 (Kastner et al., 2015), low soluble drugs (Dimov et al., 2017; Kastner et al., 2015) and combinations of  
228 high and low soluble drugs (Joshi et al., 2016). To investigate this manufacturing method for the  
229 production of liposomes entrapping proteins, we first set out to identify our working parameters in  
230 terms of the effect of lipid selection, initial lipid concentration, flow rate ratio, total flow rate and  
231 manufacturing temperature (given the potential sensitivity of drugs and proteins to temperature

232 instabilities). To achieve this, four liposome formulations were prepared using phospholipids with  
233 increasing hydrocarbon tail length (and lipid phase transition temperature) i.e. PC:Chol, DMPC:Chol,  
234 DPPC:Chol and DSPC:Chol. Liposomes were produced at a 3:1 FRR and a 15 mL/min TFR and the effect  
235 of the hydrocarbon tail length of the PC on the resulting liposomes size and PDI was investigated post  
236 solvent removal (Figure 1).

237 Results in Figure 1A show that as we increase our phospholipid alkyl chain length (from PC up to DSPC)  
238 we see a trend of decreasing vesicle size. This trend of decreasing liposome size with increasing alkyl  
239 chain length is evident across all concentrations tested (from 0.3 mg/mL to 10 mg/mL; Figure 1A). For  
240 example, at the lowest lipid concentration tested (0.3 mg/mL initial concentration) liposomes reduced  
241 significantly ( $p < 0.05$ ) from approximately 100 nm down to 60 nm in size. At the highest lipid  
242 concentration (10 mg/mL), the reduction was less notable but still significant ( $p < 0.05$ ) with liposomes  
243 reducing from 70 to 45 nm (Figure 1A). Figure 1A also shows that with increasing initial lipid  
244 concentrations, liposome size also decreases irrespective of the lipid selected (Figure 1A); as we  
245 increase from 0.3 to 10 mg/mL initial lipid concentration, PC liposomes reduce from approximately  
246 100 nm to 70 nm, DMPC liposomes reduce from 75 to 60 nm, DPPC liposomes reduce from 70 to 45  
247 nm, and DSPC liposomes reduce from 55 to 45 nm; Figure 1A). This link between lipid concentration  
248 and liposome size is in line with previously reported studies (Joshi et al., 2016) where we investigated  
249 PC:Chol liposomes. In Figure 1A we now demonstrate this effect applies to a range of liposome  
250 formulations and the lipid recovery after microfluidic production was also high (>94%) for all 4  
251 formulations tested (Table 2).

252 To consider if the reduction in vesicle size was related to lipid alkyl chain length or lipid transition  
253 temperature, we also compared liposomes prepared using two lipids with the same alkyl chain length  
254 (18 carbons) but different transition temperatures: DSPC ( $T_m$  of 55°C) and DOPC ( $T_m$  of -17°C). Table  
255 3 shows that liposomes formed using DOPC were approximately 40 nm larger in size than DSPC. This  
256 suggests that whilst adopting longer alkyl chain length PCs within the liposome formulation can reduce  
257 vesicle size, the degree of saturation and the ability of these PC to pack within a bilayer must also be  
258 considered. Irrespective of the lipid concentration, the lipid transition temperature and lipid alkyl  
259 chain length, all liposome formulations were produced with low PDI values (<0.2; Figure 1B)  
260 demonstrating the highly homogenous nature of the liposomal products produced via microfluidics.  
261 Thus, across all formulations, liposomes could easily be formulated to sizes below 100 nm with low  
262 PDI values.

263 Generally in the production of liposomes using lipid-hydration methods, liposomes must be formed  
264 above their transition temperature (Szoka Jr and Papahadjopoulos, 1980) with for example DSPC

265 liposomes commonly being prepared above 55°C. This can present issues for thermo-labile drugs and  
266 proteins. However, the addition of 50% mol/mol cholesterol has been shown by differential scanning  
267 calorimetry to abolish the gel-to-liquid phase transition temperature of DSPC liposomes (Moghaddam  
268 et al., 2011). To investigate if such increased temperatures are required for liposome production using  
269 microfluidics, we prepared various DSPC liposome formulations with increasing cholesterol  
270 concentrations (from 10:1 to 10:5 wt/wt ratio equivalent to 5 to 50 mol%; initial lipid concentration  
271 of 4 mg/mL) at a range of process temperatures (controlled within the Nanoassemblr™) from room  
272 temperature to 60°C (Figure 1C and 1D). The results demonstrate that all liposome formulations could  
273 be prepared at room temperature with no impact on the liposome size, irrespective of the transition  
274 temperature of the cholesterol concentration or the main PC lipid (in this case 55°C). The key factor  
275 controlling the liposomes size across these formulations is the cholesterol content (Figure 1C);  
276 increasing cholesterol content reduces liposome size from approximately 150 nm (10:1 wt/wt ratio)  
277 down to around 50 nm when equimolar DSPC:Cholesterol is employed as the formulation. Again whilst  
278 the formulation composition was shown to impact on the liposome size, there was no impact on the  
279 homogenous nature of the liposome suspensions with all formulations showing PDI values below 0.2  
280 (Figure 1D). These results demonstrate liposome formulations with a range of transition temperatures  
281 can be prepared using microfluidics without employing heating thereby circumventing any concerns  
282 of heat-induced degradation of the drug/lipids being incorporated.

283 The ability to manufacture liposomes from high transition temperature lipids without the need to  
284 work above the phase transition temperature of the lipids is a strong attribute of this manufacturing  
285 method as it circumvents risks of thermo-instability issues. The ability to manufacture liposomes at  
286 room temperature, irrespective of the transition temperature of the lipids incorporated, may result  
287 from the rapid 'bottom up process' of microfluidics. In this process, the liposomes are formed from  
288 individual monomers, thus the phase transition of the lipids in the bilayer does not influence the  
289 process compared to other methods where lipids need to be hydrated into liposomes and bilayers  
290 need to break-down and reform. Whilst the presence of cholesterol in formulations can help with this  
291 process by reducing transition temperature of the bilayer, this is generally only at molar  
292 concentrations of 50 % (Moghaddam et al., 2011). Cholesterol is commonly incorporated into  
293 liposomal formulations due to its well documented ability to enhance the stability of the vesicles and  
294 reduce drug leakage and membrane permeability, as first reported by Gregoriadis and Davis, (1979).  
295 Cholesterol enhances the stability of liposome bilayers by increasing the packing densities of the  
296 phospholipids (Semple et al., 1996) due to the cholesterol packing within molecular cavities formed  
297 by the lipid molecules as they arrange in the bilayer (Devaraj et al., 2002). This space-filling action of  
298 cholesterol thereby results in a more compact bilayer (Epand et al., 2003). This increased packaging

299 of the lipids and compact bilayer maybe the driver behind the smaller liposome sizes produced at  
300 higher cholesterol concentrations (Figure 1C). As mentioned, the addition of 50% mol/mol cholesterol  
301 has been shown by differential scanning calorimetry to abolish the gel-to-liquid phase transition  
302 temperature of DSPC liposomes (Moghaddam et al., 2011). However, at all concentrations tested (5  
303 to 50% mol/mol; Figure 1C and D), liposomes can be manufactured without the need to work at  
304 temperatures above the transition temperature of the main (DSPC) lipid. This confirms that the  
305 bottom-up building of the liposomes from monomers during the microfluidic process negates the  
306 need for heating during the production of liposomes irrespective of their lipid transition temperature.  
307 The initial solubility of the lipids in solvents may still be a consideration for some formulations and can  
308 be improved via adopting increased temperatures. However, across all the formulations and  
309 concentrations tested within these studies no heating was required in the processes.

310 Given that our results demonstrate both the initial lipid concentration and lipid choice impact on the  
311 size of liposomes formed, we further investigated the impact of the flow rate ratio at which we mix  
312 our solvent and aqueous phases during liposome production. Figure 2A to C demonstrate the effect  
313 of initial lipid concentration and flow rate ratio on the size and PDI of liposomes formed from  
314 DSPC:Chol (10:5 wt/wt). As can be seen, a flow rate ratio of 1:1 can be used to form larger liposomes  
315 (100 to 200 nm depending on the initial lipid concentration selected; Figure 2A) compared to the 3:1  
316 and 5:1 mixing flow rate (Figure 2B and C respectively). These larger liposomes formed at the 1:1 flow  
317 rate are not linked to an increasingly heterogeneous liposomes population as in all cases the PDI  
318 remains low ( $\leq 0.2$ ; Figure 2A). By increasing the flow rate ratio to 3:1, we can produce liposomes in a  
319 smaller size range (50 to 60 nm) again with a low PDI ( $\leq 0.2$ ) (Figure 2B). When working at 5:1 flow  
320 ratios, we tend to see more heterogeneous populations with slightly higher PDI values unless higher  
321 initial lipid concentrations are used (above 2 mg/mL; Figure 2C). Given these results, we also  
322 considered the normal operating range for anionic liposomes (DSPC:Chol:PS; 10:5:4 wt/wt) (Figure  
323 2D). From these results we see that at a 3:1 flow ratio, liposomes of 50 to 60 nm are produced across  
324 the range of concentrations tested with initial lipid concentrations of 2 mg/mL and above giving us  
325 PDI values of  $< 0.2$  (Figure 2D). We further considered the rate at which we could produce our  
326 liposomes by considering flow rates of 5 to 20 mL/min. Figure 2E and 2F confirms we can produce  
327 liposomes within the same size range and low PDI at a range of flow rates with no significant difference  
328 between the batches produced. These results demonstrate we can apply similar operating parameters  
329 for both neutral and anionic formulations and achieve highly reproducible and homogenous liposome  
330 formulations.

331 Previous studies by Kastner et al using liposomal formulation DOPE:DOTAP and PC:Chol on a staggered  
332 herringbone micromixer chip show a reduction in average liposome size as the flow rate ratio was

333 increased from 1:1 to 5:1. The average liposome size of the formulations at a flow rate ratio of 1:1  
334 resulted in sizes above 200 nm, while a flow rate ratio of 5:1 generated sizes around 50 nm (Kastner  
335 et al., 2014) (Kastner et al., 2015). Similar results were obtained by Jahn et al where the authors  
336 showed that as the flow rate ratio was increased, the resulting particle size decreased. This was  
337 attributed to the difference in the alcohol content of the flow rate ratios, as the flow rate ratio  
338 decreases the amount of alcohol injected into the stream increases. When the lipids in alcohol first  
339 come in contact with the aqueous stream, liposomes will self-assemble and form at the interface. As  
340 the streams then continue to mix, the initially formed liposomes take alcohol up and reach the critical  
341 alcohol concentration resulting in some partial disassembly, the continuing mixing will then decrease  
342 the alcohol concentration in the liposomes again, resulting in re-assembly. When the flow rate ratio is  
343 increased, the overall alcohol concentration is reduced, thus the amount of liposomes exposed to  
344 fluctuating increases and decreases of alcohol is reduced thus limiting the assembly / re-assembly  
345 cycle (Jahn et al., 2010) (Jahn et al., 2007). Similar findings were also reported by Zizzari et al for the  
346 liposomal formulation HSPC:Chol:mPEG-2000-DSPE produced over a range of flow rate ratios. Again,  
347 Zizzari et al note that at higher flow rate ratios, a smaller solvent stream results and as the lipid discs  
348 form at the liquid interface they begin to bend, eventually forming a vesicular particle as a result of  
349 surface area of the hydrophobic chains in the presence of decreasing solvent concentration. The  
350 length of time these lipid discs are allowed to grow will directly impact upon the final vesicle size, with  
351 shorter times leading to smaller liposomes. Thus at lower flow rate ratios (e.g. 1:1), the higher the  
352 concentration of solvent and thus the longer the time the lipid discs have to expand (Zizzari et al.,  
353 2017). Whilst the flow rate ratio has been shown to impact upon liposome size and thus should be  
354 tested to identify the normal operating range for a given formulation, the total flow rate (TFR mL/min)  
355 did not impact on the liposome size and with the formulations tested a flow rate of 5 to 20 mL/min is  
356 a proven acceptable range to work within. This is in line with previous work reported by Joshi et al  
357 where again the flow ratio was shown to impact on particle size of PC:Chol liposomes, but flow rate  
358 had no impact across all speeds tested (Joshi et al., 2016). Therefore, we have established that by  
359 choosing the appropriate initial lipid concentration in the tested range of flow rates, we can control  
360 liposome size and maintain low (<0.2) PDI values through selection of flow ratios in combination with  
361 the initial lipid concentration. For all formulations, a heating step can be eliminated circumventing any  
362 potential thermal protein denaturation occurring.

### 363 **3.2 Purification and concentration of liposomal systems.**

364 To ensure removal of residual solvent and non-incorporated protein, liposomes were purified via  
365 tangential flow filtration (TFF). To validate the purification process and confirm solvent removal,  
366 residual solvent levels were quantified via headspace gas chromatography (Figure 3A). Results show

367 that after 12 wash cycles solvent levels were below ICH guidelines of less than 3000 parts per million  
368 (or less than 0.3% of residual solvent remaining) (International conference in Harmonisation, 2016  
369 (ICH)). Similarly, this wash cycle was able to remove all non-incorporated protein (Figure 3B). This was  
370 confirmed by mixing pre-prepared 'empty' liposomes and with various protein concentrations. Given  
371 the protein was not entrapped, 100% removal confirms all free protein can be removed. Figure 3C,  
372 confirms the TFF process has no detrimental effect on the liposome attributes with the particle size,  
373 PDI and morphology remaining unchanged, and liposome recovery was high (95-100%; results not  
374 shown).

375 Using TFF, we were also able to concentrate both the neutral (Figure 4A and B) and anionic liposome  
376 formulations (Figure 4C and D) up to 4 fold, without any detriment to their vesicle attributes with four  
377 cycles being sufficient to double the concentration of liposomes. The recovery of the liposomes was  
378 again 95-100% (results not shown) similar to studies where a lab-on-chip TFF purification system was  
379 adopted (Dimov et al., 2017). The ability to purify liposome formulations in a scalable format is an  
380 important feature of any manufacturing process. Furthermore, the lipid solubility of some lipids within  
381 suitable solvents can be limited and thus TFF can allow the concentration of liposome formulations to  
382 required doses. These studies demonstrate the ability to purify and/or concentrate liposome  
383 formulations in scalable format.

### 384 **3.3 Scale-independent manufacturing of liposomes entrapping proteins.**

385 Now that we have identified the normal operating range for the microfluidic production and  
386 appropriate purification protocols for a range liposome formulations, we can next consider protein  
387 loading of these liposomes. First, we compared protein loading of liposomes composed of DSPC:Chol  
388 (10:5 wt/wt) prepared by microfluidics, sonication and extrusion. Liposomes produced by  
389 microfluidics gives high protein loading (25 – 35%; 250 µg/mL initial protein concentration), whilst  
390 both sonication and extrusion gave low (< 5%) protein loading (Figure 5A). Microfluidics also produced  
391 small vesicles (60 to 70 nm; PDI 0.2) similar in size to 'empty' liposomes and notably smaller and more  
392 homogeneous than vesicles formed from sonication or extrusion (Figure 5A). The similarity in size  
393 between loaded and unloaded liposomes suggests that in the initial process development, empty  
394 liposomes can be used, reducing the amount (and cost) of active pharmaceutical ingredient used.

395 The effect of extrusion on protein loaded MLVs has previously been shown to reduce the  
396 concentration of protein entrapped within the vesicles following extrusion cycles. Large particles that  
397 cannot flow through are blocked at the membrane pores and the pressure from the extrusion process  
398 ruptures the liposomes (Patty and Frisken, 2003). This rupturing coincides with a major decrease in  
399 the encapsulation efficiency of the protein after the first extrusion cycle and the retention of the

400 protein upon the filter (Colletier et al., 2002). This presents protein entrapment issues if progressively  
401 smaller and smaller membrane filters are used during the extrusion process to downsize MLVs to size  
402 ranges below 100 nm (which are easily achieved via microfluidics). Similarly, probe sonication of  
403 liposome formulations for size reduction leads to poor encapsulation efficiencies, generally below 10  
404 % for aqueous soluble macromolecules (Lapinski et al., 2007). Although sonication is widely used to  
405 break down MLVs by acoustic energy (Mendez and Banerjee, 2017), there is little control of the end  
406 product with batch to batch variation. A lack of temperature control can also present challenges for  
407 protein encapsulation, and depending on the system, the need to remove contamination post  
408 sonication is an added step to production (Philippot and Schuber, 2017). In comparison, the rapid  
409 production processes, coupled with higher encapsulation efficiencies of protein, demonstrates that  
410 microfluidics is an effective method for one step, scalable production of protein loaded liposomes.

411 When produced via microfluidics, the choice of lipid used within the liposome formulation has no  
412 significant impact on protein loading with liposomes composed of PC, DMPC, DPPC and DSPC all  
413 showing similarly high (30-40%) protein loading (Figure 5B). These formulations were prepared at  
414 room temperature and Figure 5C shows that the ovalbumin (OVA) contained in liposomes and the  
415 untreated OVA have a similar CD spectra. In addition, the CD spectrum, containing information on the  
416 OVA structure, with nine alpha helical structures and two beta sheets (Stein et al., 1990), is in keeping  
417 with literature (Paolinelli et al., 1997). Therefore, it is concluded from the CD measurements that the  
418 entrapped protein retained its structural conformation during liposome production.

419 We again investigated the influence of lipid concentration on these systems, this time in relation to  
420 protein encapsulation. Varying amounts of PC, DMPC, DPPC and DSPC liposomes (from 0.5 to 10  
421 mg/mL initial lipid concentration) were used and the encapsulation efficiency of OVA (250 µg/mL)  
422 tested. This was plotted on a double logarithmic plot of the encapsulation versus lipid concentration  
423 as previously done by Colletier et al. (Colletier et al., 2002) (Figure 5D). The authors suggest to do this  
424 as the total liposome surface area is proportional to the lipid concentration, yet the encapsulated  
425 inner volume is proportional to the lipid concentration to the power 3/2. Thus the double log plot  
426 allows the discrimination between the relevant parameters (Colletier et al., 2002). With all 4 liposome  
427 formulations, the data shows a relatively good linear correlation ( $R^2 > 0.9$ ). It has been proposed that  
428 if the gradient is close to 1 then encapsulation is proportional to the number of lipids and the surface  
429 area, and if the slope is close to 1.5 this suggest that encapsulation is related to internal volume. Whilst  
430 the plot of DMPC:Chol can be seen to have a gradient close to 1, PC, DPPC and DSPC are notable lower  
431 than 1 and all 4 are far from 1.5. This suggests that the high incorporation of protein within liposomes  
432 using microfluidics is a factor of the manufacturing process and less influenced by the number of lipids  
433 or by the internal volume.

434 We further studied the protein loading efficiency of both neutral (DSPC:Chol; 10:5 wt/wt) and anionic  
435 (DSPC:Chol:PS; 10:5:4 wt/wt) liposomes at a fixed lipid concentration and increasing protein  
436 concentrations. Figure 6A shows that up to an initial protein concentration of 2 mg/mL protein  
437 encapsulation efficiency remains high at approximately 30 %, which is equivalent to approximately  
438 400 µg/mL prior to any concentration steps. Over this protein concentration range, the liposome size  
439 and PDI remained stable at around 60 – 80 nm and PDI of ~0.2 (Figure 6B), with a near neutral zeta  
440 potential (Figure 6C). Increasing the protein concentration further, to 10 mg/mL, caused a drop in  
441 encapsulation efficiency (15%) but an increase in the total amount of OVA loaded. However, it also  
442 resulted in aggregation and large particle sizes (above 700 nm; results not shown). Anionic liposomes  
443 (Figure 6D – F) also gave good protein loading over the same range (0.1 to 2 mg/mL initial protein  
444 concentrations) with entrapment efficiencies of ~ 20 % (Figure 6D) and the protein loading within the  
445 liposomes does not influence their particle size, PDI nor zeta potential over this range (Figure 6E and  
446 F).

447 The decrease in entrapment efficiency with the anionic liposomal formulation compared to the  
448 neutral formulation is not un-common. Colletier et al also investigated the effect of charge on the  
449 entrapment efficiencies of acetylcholinesterase using a neutral lipid POPC and an anionic lipid POPS.  
450 Using multiple freeze-thaw cycles, the anionic formulation achieved an encapsulation efficiency  
451 around 20% while the neutral POPC formulation achieved around 40% acetylcholinesterase  
452 encapsulation indicating the electrostatic interactions between proteins peripheral charge and the  
453 polar head group of the phospholipids has a substantial control over the ability of the entrapment  
454 process within the vesicles (Colletier et al., 2002).

455 The effect of flow ratio and flow rate was also considered for both these liposome formulations (Figure  
456 7). Only flow rates of 3:1 and 5:1 were considered as a flow ratio of 1:1 was shown to result in  
457 aggregation which may be a result of protein aggregation at high (50%) solvent concentrations (results  
458 not shown). Increasing the flow rate from 3:1 to 5:1 was shown to reduce protein loading by  
459 approximately 10% and increasing the variability in the particle size of the DSPC:Chol liposomes (Figure  
460 7A and B respectively). Working at flow rate of 10 mL/min or above also gave reproducible protein  
461 loading (20 – 25%; 700 µg/mL initial ovalbumin concentration), particle size (55 – 65 nm) and PDI (~0.2)  
462 (Figure 7C and D). This is again comparable to our data with empty liposomes (Figure 2). Similar results  
463 were shown with the anionic liposomes (DSPC:Chol:PS); increasing the flow rate ratio from 3:1 to 5:1,  
464 significantly ( $p < 0.05$ ) reduced protein loading from 20% to 9% (Figure 7E) without influencing  
465 liposome size (100 – 110 nm; Figure 7F). Again working at a flow rates of 10 mL/min or more giving  
466 protein loading of 20 – 25 % with no significant impact on protein loading (Figure 7G) nor particle size  
467 (which remained around 100 to 120 nm; Figure 7H). With both formulations, working a low flow rate

468 of 5 mL/min did reduce protein loading despite particle size remaining the same. This again suggests  
469 that protein entrapment efficiency is controlled more by the manufacturing than the lipid/protein  
470 concentrations and thus can be easily scaled within identified normal operating ranges.

471 In order to determine the effect of flow rate ratio on the protein encapsulation efficiency, the final  
472 lipid and protein concentrations described in figure 7 were matched by adjusting the initial  
473 concentrations. Despite controlling for these variables, a significantly lower protein entrapment  
474 efficiency is observed when the flow rate ratio is increased from 3:1 to 5:1. The difference in  
475 encapsulation efficiency between the flow rate ratios could be due a shift in position of the liquid-  
476 liquid interface between the two different flow rate ratios during liposome production in the chip  
477 (Oellers et al., 2017). At a 1:1 FRR the liquid-liquid interface (the mixing of the solvent and aqueous  
478 phase) occurs at the centre of the chip, with this position changing in accordance to the FRR selected.  
479 Carugo et al also note that changes in the flow rate ratio have a direct impact upon the fluid stream,  
480 thus altering the properties of the fluidic environment within the chip which could impact upon the  
481 interactions between the lipid phase and aqueous protein during liposomal formation (Carugo et al.,  
482 2016).

483 Given the various parameters for optimal loading have been established, these parameters were then  
484 tested with two additional proteins (Table 4) and in a 10 times scaled process (Figure 8). Table 4  
485 demonstrates that both a smaller protein (insulin) and larger protein (bovine serum albumin) can also  
486 be effectively entrapped (25 to 37 %) within DSPC:Chol liposomes prepared using the optimised  
487 parameters, with liposomes in a similar size range (55 - 70 nm) being produced. Furthermore, to  
488 demonstrate the scalability of the process, two batches of liposomes (DSPC:Chol) were prepared by  
489 either the small-laboratory scale NanoAssemblr® Benchtop (1 -15 mL batch size) and the larger Blaze™  
490 (10 mL to 1 L batch size) entrapping OVA. Across both platforms, liposomes were manufactured with  
491 reproducible results in terms of protein loading and particle attributes (Figure 8), demonstrating the  
492 easy scale-up of the process developed.

### 493 **3.4 Release characteristics of liposomes entrapping protein**

494 The ability of liposome formulations to retain, delivery and release protein is important. Release  
495 profiles of protein in-vitro can be used to determine behaviour in vivo. The release rate of protein  
496 from liposomes is highly dependent on factors such as liposome composition and the nature of the  
497 protein entrapped (Panagi et al., 1998). The effect of liposome composition was investigated using  
498 four neutral liposomes containing cholesterol. Lipids with varying carbon chain lengths were tested to  
499 investigate the effect of tail length on release. Figure 9A shows all four neutral formulations (PC:Chol,  
500 DMPC:Chol, DPPC:Chol and DSPC:Chol) are capable of protein release. The general trend observed

501 confirms previous research whereby, the longer hydrocarbon tailed lipids used the slower the release  
502 (e.g. Panagi et al., 1998). OVA is fully released from PC:Chol liposomes within 72 hours, meanwhile  
503 both DPPC:Chol and DSPC:Chol do not fully release OVA by 120 hours; there is 9% OVA remaining for  
504 DPPC:Chol and 47% OVA remaining for the DSPC:Chol liposomes after 5 days. The findings are in  
505 keeping with previous studies showing liposomes formulated from longer chain lipids have slower  
506 release rates due to their increased bilayer rigidity. Longer chain lipids, such as DSPC, have more  
507 opportunity to create Van der Waals forces between the longer hydrocarbon tails and improved  
508 membrane packing compared to liposomes composed of shorter chain phosphatidylcholines  
509 (Mohammed et al., 2004; Panagi et al., 1998). Moreover, the release profiles for PC:Chol, DMPC:Chol  
510 and DPPC:Chol liposomes prepared by microfluidics match previous studies whereby a burst release  
511 is observed within the first 12 hours, after which a slower rate of release is observed (Monteiro et al.,  
512 2014; Murao et al., 2002; Panagi et al., 1998).

513 In addition, given the ability to manipulate the flow rate ratio to change liposomal formulation  
514 characteristics, the effect of this ratio on protein release from liposomes was investigated. Two  
515 formulations (DMPC:Chol and DSPC:Chol) were used to investigate any possible changes in release  
516 caused by the selected manufacturing process. The encapsulation efficiency for DMPC:Chol liposome  
517 formulations produced at a 3:1 FRR is  $37 \pm 0.2$  % and  $29 \pm 0.6$  % for DMPC:Chol liposomes produced  
518 at a 5:1 FRR. Figure 9B shows the 5:1 FRR releases the protein OVA at a faster rate in comparison to  
519 the DMPC:Chol liposomes produced at a 3:1 FRR with a similarity factor ( $f_2$ ) of 24.6 being calculated  
520 (it is generally accepted that an  $f_2$  of 50-100 suggests similar release profiles). The same pattern is also  
521 observed for OVA loaded DSPC:Chol liposomes produced at a 3:1 and 5:1 FRR (Figure 8C), with the  
522 DSPC:Chol liposomes produced at a 5:1 showing a faster release rate ( $f_2$  of 48.3) than DSPC:Chol  
523 liposomes produced at 3:1 despite the amount of protein loaded within these formulations being  
524 matched (0.1875 ug/mL final OVA concentration). Similar to the differences noted in encapsulation  
525 efficiency of the liposomes produced by FRRs, a range of factors may be responsible for the effect of  
526 flow rate ratio on release rate. As previously mentioned, when the flow rate ratio is increased, the  
527 alcohol concentration is reduced, which reduces the opportunity for liposomes to re-assemble during  
528 their production (Jahn et al., 2010) (Jahn et al., 2007). Also at lower alcohol concentrations, there is  
529 less time for lipid discs to expand and form liposomes (Zizzari et al., 2017); different flow rate ratios  
530 result in a shift in position of the liquid-liquid interface (Oellers et al., 2017). Each or all of these factor  
531 may impact on the assembly of the liposomal bilayers which in turn will impact on release profiles. A  
532 shift in the position of the liquid-liquid interface and/or differences in the ethanol concentrations  
533 could result in subtle changes in the cholesterol tilt within the liposome bilayers. Indeed, the position  
534 of cholesterol is highly variable with concentration and production method used. Research by

535 Khelashvili and Harries (Khelashvili and Harries, 2013; Khelashvili et al., 2010), has shown that  
536 DMPC:Chol liposomes with a cholesterol concentration of more than 30%, preferred an upright  
537 position so it is more aligned to the phospholipid bilayer (Khelashvili and Harries, 2013). Therefore, in  
538 the bottom up process, the solvent concentration at the point of formation may impact of the  
539 orientation/alignment of cholesterol thus impacting on protein release. This manufacturing  
540 parameter controlled change in release profile, further demonstrating microfluidic is a versatile  
541 system. It can be fine-tuned to modify liposome attributes and the flow rate ratio is a key quality  
542 attribute which influences particle size, protein loading and protein release.

### 543 **3.5 Continuous manufacture with at-line size analysis**

544 High-throughput production of liposomes using microfluidics requires an ability to monitor liposome  
545 attributes during manufacturing. In particular, liposome size is a key product attribute given the  
546 impact this can have on drug loading, drug release and biodistribution. Therefore, the ability to  
547 monitor liposome size rapidly during production is a key element of a manufacturing process. To  
548 achieve this, we incorporated at-line (in real time) particle size monitoring using the Malvern Zetasizer  
549 AT (Malvern Instruments, Malvern, UK) both for in-process monitoring and for product validation  
550 (Figure 10). The sensitivity of this instrument was compared to the off-line characterising equipment  
551 (the Zetasizer Nano ZS) and two monitoring points in the production of DSPC:Chol liposomes were  
552 tested: in-process (directly after production) and the final purified product. The results in figure 10  
553 confirm that the liposome size can be effectively monitored in real time (at-line) at both points in the  
554 process. After production, the liposome sizes recorded were  $49 \pm 0.4$  nm when measured at-line  
555 compared with  $50 \pm 0.3$  nm when measured off-line. Similarly, after purification, the final liposome  
556 product particle size was  $52 \pm 0.4$  nm when measured at-line compared with  $52 \pm 0.7$  nm when  
557 measured off-line. There was also no significant difference in the PDI measured by both instruments  
558 after microfluidics ( $\sim 0.06$  PDI) and post purification ( $\sim 0.15$  PDI), thus indicating a rapid at-line particle  
559 size analysis can be incorporated within this continuous and scalable-independent process for  
560 monitoring liposomal formulation quality in real-time.

### 561 **4. Conclusions**

562 We have successfully shown for the first time, a simple and scale-independent method to  
563 manufacture, purify and monitor the production of liposomes encapsulating proteins. This process  
564 gives high protein loading and can be undertaken at room temperature thereby circumventing any  
565 potential risk to the protein structure. Key process parameters identified are the lipid concentration,  
566 the liposome composition, the protein concentration and the flow rate ratio. This microfluidic  
567 manufacturing process ensures a quick and efficient process for the translation of novel liposome

568 formulations from the bench to production and de-risks the adoption of liposomes for wide-scale  
569 applications.

## 570 **5. Acknowledgements**

571 This work was part funded by the EPSRC Centre for Innovative Manufacturing in Emergent Therapies  
572 (EPSRC) and the University of Strathclyde. We would like to thank Malvern Panalytical for the use of  
573 the Zetasizer AT. JtH and MLB thank the EPSRC Centre for Innovative Manufacturing in Continuous  
574 Manufacturing and Crystallisation (<http://www.cmac.ac.uk>) for support (EPSRC funding under grant  
575 reference: EP/I033459/1).

## 576 **6. Supporting information Available**

577 Data presented in this publication can be found at [DOI to be confirmed on acceptance of manuscript].

578 **References**

- 579 Bulbake, U., Doppalapudi, S., Kommineni, N., Khan, W., 2017. Liposomal Formulations in Clinical Use:  
580 An Updated Review. *Pharmaceutics* 9, 12.
- 581 Carter, P.J., 2011. Introduction to current and future protein therapeutics: A protein engineering  
582 perspective. *Experimental Cell Research* 317, 1261-1269.
- 583 Carugo, D., Bottaro, E., Owen, J., Stride, E., Nastruzzi, C., 2016. Liposome production by microfluidics:  
584 potential and limiting factors. *Scientific reports* 6.
- 585 Chan, Y.-H., Chen, B.-H., Chiu, C.P., Lu, Y.-F., 2004. The influence of phytosterols on the encapsulation  
586 efficiency of cholesterol liposomes. *International Journal of Food Science & Technology* 39, 985-995.
- 587 Colletier, J.-P., Chaize, B., Winterhalter, M., Fournier, D., 2002. Protein encapsulation in liposomes:  
588 efficiency depends on interactions between protein and phospholipid bilayer. *BMC biotechnology* 2,  
589 9.
- 590 Devaraj, G.N., Parakh, S., Devraj, R., Apte, S., Rao, B.R., Rambhau, D., 2002. Release studies on  
591 niosomes containing fatty alcohols as bilayer stabilizers instead of cholesterol. *Journal of colloid and*  
592 *interface science* 251, 360-365.
- 593 Dimov, N., Kastner, E., Hussain, M., Perrie, Y., Szita, N., 2017. Formation and purification of tailored  
594 liposomes for drug delivery using a module-based micro continuous-flow system. *Scientific reports* 7,  
595 12045.
- 596 Epand, R.M., Epand, R.F., Maekawa, S., 2003. The arrangement of cholesterol in membranes and  
597 binding of NAP-22. *Chemistry and physics of lipids* 122, 33-39.
- 598 Fatouros, D.G., Antimisariaris, S.G., 2002. Effect of amphiphilic drugs on the stability and zeta-potential  
599 of their liposome formulations: a study with prednisolone, diazepam, and griseofulvin. *Journal of*  
600 *colloid and interface science* 251, 271-277.
- 601 Fosgerau, K., Hoffmann, T., 2015. Peptide therapeutics: current status and future directions. *Drug*  
602 *Discovery Today* 20, 122-128.
- 603 Gregoriadis, G., Davis, C., 1979. Stability of liposomes *in vivo* and *in vitro* is promoted by their  
604 cholesterol content and the presence of blood cells. *Biochemical and Biophysical Research*  
605 *Communications* 89, 1287-1293.
- 606 Gregoriadis, G., Leathwood, P., Ryman, B.E., 1971. Enzyme entrapment in liposomes. *FEBS letters* 14,  
607 95-99.
- 608 Habjanec, L., Frkanec, R., Halassy, B., Tomašić, J., 2006. Effect of liposomal formulations and  
609 immunostimulating peptidoglycan monomer (PGM) on the immune reaction to ovalbumin in mice.  
610 *Journal of liposome research* 16, 1-16.
- 611 Huang, Y.-Y., Wang, C.-H., 2006. Pulmonary delivery of insulin by liposomal carriers. *Journal of*  
612 *Controlled Release* 113, 9-14.
- 613 ICH, I., Q3C (R6) Impurities: Guideline for Residual Solvents. 2016. There is no corresponding record  
614 for this reference.
- 615 Jahn, A., Stavis, S.M., Hong, J.S., Vreeland, W.N., DeVoe, D.L., Gaitan, M., 2010. Microfluidic Mixing  
616 and the Formation of Nanoscale Lipid Vesicles. *ACS Nano* 4, 2077-2087.
- 617 Jahn, A., Vreeland, W.N., DeVoe, D.L., Locascio, L.E., Gaitan, M., 2007. Microfluidic Directed Formation  
618 of Liposomes of Controlled Size. *Langmuir* 23, 6289-6293.
- 619 Joshi, S., Hussain, M.T., Roces, C.B., Anderluzzi, G., Kastner, E., Salmaso, S., Kirby, D.J., Perrie, Y., 2016.  
620 Microfluidics based manufacture of liposomes simultaneously entrapping hydrophilic and lipophilic  
621 drugs. *International journal of pharmaceutics* 514, 160-168.
- 622 Kastner, E., Kaur, R., Lowry, D., Moghaddam, B., Wilkinson, A., Perrie, Y., 2014. High-throughput  
623 manufacturing of size-tuned liposomes by a new microfluidics method using enhanced statistical tools  
624 for characterization. *International Journal of Pharmaceutics* 477, 361-368.
- 625 Kastner, E., Verma, V., Lowry, D., Perrie, Y., 2015. Microfluidic-controlled manufacture of liposomes  
626 for the solubilisation of a poorly water soluble drug. *International journal of pharmaceutics* 485, 122-  
627 130.

628 Khelashvili, G., Harries, D., 2013. How sterol tilt regulates properties and organization of lipid  
629 membranes and membrane insertions. *Chemistry and Physics of Lipids* 169, 113-123.

630 Khelashvili, G., Pabst, G., Harries, D., 2010. Cholesterol orientation and tilt modulus in DMPC bilayers.  
631 *The Journal of Physical Chemistry B* 114, 7524-7534.

632 Lapinski, M.M., Castro-Forero, A., Greiner, A.J., Ofoli, R.Y., Blanchard, G.J., 2007. Comparison of  
633 liposomes formed by sonication and extrusion: rotational and translational diffusion of an embedded  
634 chromophore. *Langmuir* 23, 11677-11683.

635 Lee, K.Y., Yuk, S.H., 2007. Polymeric protein delivery systems. *Progress in Polymer Science* 32, 669-  
636 697.

637 Li, N., Peng, L.-H., Chen, X., Nakagawa, S., Gao, J.-Q., 2011. Effective transcutaneous immunization by  
638 antigen-loaded flexible liposome in vivo. *International Journal of Nanomedicine* 6, 3241-3250.

639 Liu, W., Ye, A., Liu, W., Liu, C., Han, J., Singh, H., 2015. Behaviour of liposomes loaded with bovine  
640 serum albumin during in vitro digestion. *Food Chemistry* 175, 16-24.

641 Lu, Y., Sun, W., Gu, Z., 2014. Stimuli-Responsive Nanomaterials for Therapeutic Protein Delivery.  
642 *Journal of controlled release : official journal of the Controlled Release Society* 194, 1-19.

643 Mendez, R., Banerjee, S., 2017. Sonication-based basic protocol for liposome synthesis. *Lipidomics:  
644 Methods and Protocols*, 255-260.

645 Moghaddam, B., Ali, M.H., Wilkhu, J., Kirby, D.J., Mohammed, A.R., Zheng, Q., Perrie, Y., 2011. The  
646 application of monolayer studies in the understanding of liposomal formulations. *International Journal  
647 of Pharmaceutics* 417, 235-244.

648 Mohammed, A., Weston, N., Coombes, A., Fitzgerald, M., Perrie, Y., 2004. Liposome formulation of  
649 poorly water soluble drugs: optimisation of drug loading and ESEM analysis of stability. *International  
650 journal of pharmaceutics* 285, 23-34.

651 Monteiro, N., Martins, A., Reis, R.L., Neves, N.M., 2014. Liposomes in tissue engineering and  
652 regenerative medicine. *Journal of the Royal Society Interface* 11, 20140459.

653 Murao, A., Nishikawa, M., Managit, C., Wong, J., Kawakami, S., Yamashita, F., Hashida, M., 2002.  
654 Targeting efficiency of galactosylated liposomes to hepatocytes in vivo: effect of lipid composition.  
655 *Pharmaceutical research* 19, 1808-1814.

656 Oellers, M., Bunge, F., Vinayaka, P., Driesche, S.v.d., Vellekoop, M.J., 2017. Flow-Ratio Monitoring in a  
657 Microchannel by Liquid-Liquid Interface Interferometry, *Multidisciplinary Digital Publishing Institute  
658 Proceedings*, p. 498.

659 Panagi, Z., Avgoustakis, K., Evangelatos, G., Ithakissios, D., 1998. Protein-induced CF release from  
660 liposomes in vitro and its correlation with the BLOOD/RES biodistribution of liposomes. *International  
661 journal of pharmaceutics* 163, 103-114.

662 Paolinelli, C., Barteri, M., Boffi, F., Forastieri, F., Gaudiano, M.C., Della Longa, S., Castellano, A.C., 1997.  
663 Structural differences of ovalbumin and S-ovalbumin revealed by denaturing conditions. *Zeitschrift für  
664 Naturforschung C* 52, 645-653.

665 Patty, P.J., Frisken, B.J., 2003. The pressure-dependence of the size of extruded vesicles. *Biophysical  
666 journal* 85, 996-1004.

667 Philippot, J.R., Schuber, F., 2017. *Liposomes as Tools in Basic Research and Industry (1994)*. CRC press.

668 Ramaldes, G.A., Deverre, J.R., Grognet, J.M., Puisieux, F., Fattal, E., 1996. Use of an enzyme  
669 immunoassay for the evaluation of entrapment efficiency and in vitro stability in intestinal fluids of  
670 liposomal bovine serum albumin. *International Journal of Pharmaceutics* 143, 1-11.

671 Semple, S.C., Chonn, A., Cullis, P.R., 1996. Influence of cholesterol on the association of plasma  
672 proteins with liposomes. *Biochemistry* 35, 2521-2525.

673 Stein, P.E., Leslie, A.G., Finch, J.T., Turnell, W.G., McLaughlin, P.J., Carrell, R.W., 1990. Crystal structure  
674 of ovalbumin as a model for the reactive centre of serpins. *Nature* 347, 99.

675 Szoka, F., Papahadjopoulos, D., 1978. Procedure for preparation of liposomes with large internal  
676 aqueous space and high capture by reverse-phase evaporation. *Proceedings of the national academy  
677 of sciences* 75, 4194-4198.

678 Szoka Jr, F., Papahadjopoulos, D., 1980. Comparative properties and methods of preparation of lipid  
679 vesicles (liposomes). *Annual review of biophysics and bioengineering* 9, 467-508.  
680 Torchilin, V.P., Lukyanov, A.N., 2003. Peptide and protein drug delivery to and into tumors: challenges  
681 and solutions. *Drug Discovery Today* 8, 259-266.  
682 Usmani, S.S., Bedi, G., Samuel, J.S., Singh, S., Kalra, S., Kumar, P., Ahuja, A.A., Sharma, M., Gautam, A.,  
683 Raghava, G.P.S., 2017. THPdb: Database of FDA-approved peptide and protein therapeutics. *PLOS ONE*  
684 12, e0181748.  
685 Vila-Caballer, M., Codolo, G., Munari, F., Malfanti, A., Fassan, M., Rugge, M., Balasso, A., de Bernard,  
686 M., Salmaso, S., 2016. A pH-sensitive stearyl-PEG-poly(methacryloyl sulfadimethoxine)-decorated  
687 liposome system for protein delivery: An application for bladder cancer treatment. *Journal of*  
688 *Controlled Release* 238, 31-42.  
689 Xu, X., Costa, A., Burgess, D.J., 2012. Protein encapsulation in unilamellar liposomes: high  
690 encapsulation efficiency and a novel technique to assess lipid-protein interaction. *Pharmaceutical*  
691 *research* 29, 1919-1931.  
692 Zizzari, A., Bianco, M., Carbone, L., Perrone, E., Amato, F., Maruccio, G., Rendina, F., Arima, V., 2017.  
693 Continuous-Flow Production of Injectable Liposomes via a Microfluidic Approach. *Materials* 10, 1411.  
694

695 **Tables**

696 **Table 1. Examples of traditional methods used to entrap proteins within liposomes and their relative**  
 697 **entrapment efficiencies.** The efficiency of neutral and anionic liposomes to encapsulate protein was  
 698 investigated relative to the manufacturing methods.

Protein loaded	Liposome formulation	Production technique	Protein loading	Reference
<b>Bovine serum albumin</b>	soyabean PC/DSPC, cholesterol, phosphatidylglycerol	Thin film lipid hydration.	0.1 mg/mL	(Ramaldes et al., 1996)
<b>Bovine serum albumin</b>	PC:Chol	Dehydration-rehydration method.	28%	(Chan et al., 2004)
<b>Bovine Serum Albumin</b>	PC:Chol:Tween:Vitamin E	Thin film lipid hydration.	34 ± 9%	(Liu et al., 2015)
<b>Bovine Serum Albumin</b>	Soybean PC:Chol	Thin film lipid hydration.	22-32%.	(Vila-Caballer et al., 2016)
<b>Ovalbumin</b>	PC:Chol	Thin film lipid hydration.	10%	(Habjanec et al., 2006)
<b>Ovalbumin</b>	Phospholipid S, Chol (very high lipid concentration, 200 mg)	Thin film lipid hydration.	48% ± 9%	(Li et al., 2011)
<b>Amyloglucosidase, Albumin</b>	PC:Chol:Dicetylphosphate	Lipid film hydration	4 - 6.5%, 6.8 - 10.6%	(Gregoriadis et al., 1971)
<b>Superoxide dismutase</b>	DPPC:Chol DSPC:Chol	Unilamellar vesicles mixed with freeze-thaw cycling	50%	(Xu et al., 2012)
<b>Acetylcholinesterase</b>	Egg PC	Thin film lipid hydration.	35%	(Colletier et al., 2002)
<b>Insulin</b>	Hydrogenated PC:Chol	Thin film lipid hydration.	28% (4°C) 30% (25°C) and 50% (40°C)	(Huang and Wang, 2006)

699

700 **Table 2. Lipid recovery in liposomes produced by microfluidics.** Four liposomal formulations (PC:Chol,  
 701 DMPC:Chol, DPPC:Chol and DSPC:Chol each at 2:1 wt/wt) were manufactured using microfluidics at a  
 702 flow rate ratio of 3:1, 15 mL/min TFR and purified using dialysis. Lipid recovery was calculated using  
 703 HPLC-ELSD. Results represent mean ± SD, n=3 independent batches.

Formulation	Lipid recovery (% of initial amount)							
	PC:Chol		DMPC:Chol		DPPC:Chol		DSPC:Chol	
Lipid	PC	Chol	DMPC	Chol	DPPC	Chol	DSPC	Chol
Recovery	94 ± 5.0	95 ± 2.3	95 ± 1.6	96 ± 1.0	96 ± 1.2	97 ± 2.7	98 ± 5.7	97 ± 3.8

704

705 **Table 3. Comparison of particle size of liposomes formulated from phospholipids of different phase**  
 706 **transition temperatures manufactured via microfluidics.** Two liposome formulations (DSPC:Chol  
 707 (10:5 wt/wt) and DOPC:Chol (10:5 wt/wt), initial lipid concentration of 1 mg/mL) were manufactured  
 708 using microfluidics at a flow rate ratio of 3:1, 15 mL/min TFR and purified using dialysis. Results  
 709 represent mean  $\pm$  SD, n=3 independent batches.

	Carbon chain length	T <sub>m</sub> (°C)	Saturation	Particle size (nm)	PDI
DOPC	18 carbons	-17	18:1c9	84.9 $\pm$ 4.3	0.13 $\pm$ 0.04
DSPC	18 carbons	55	18:0	41.5 $\pm$ 0.2	0.03 $\pm$ 0.01

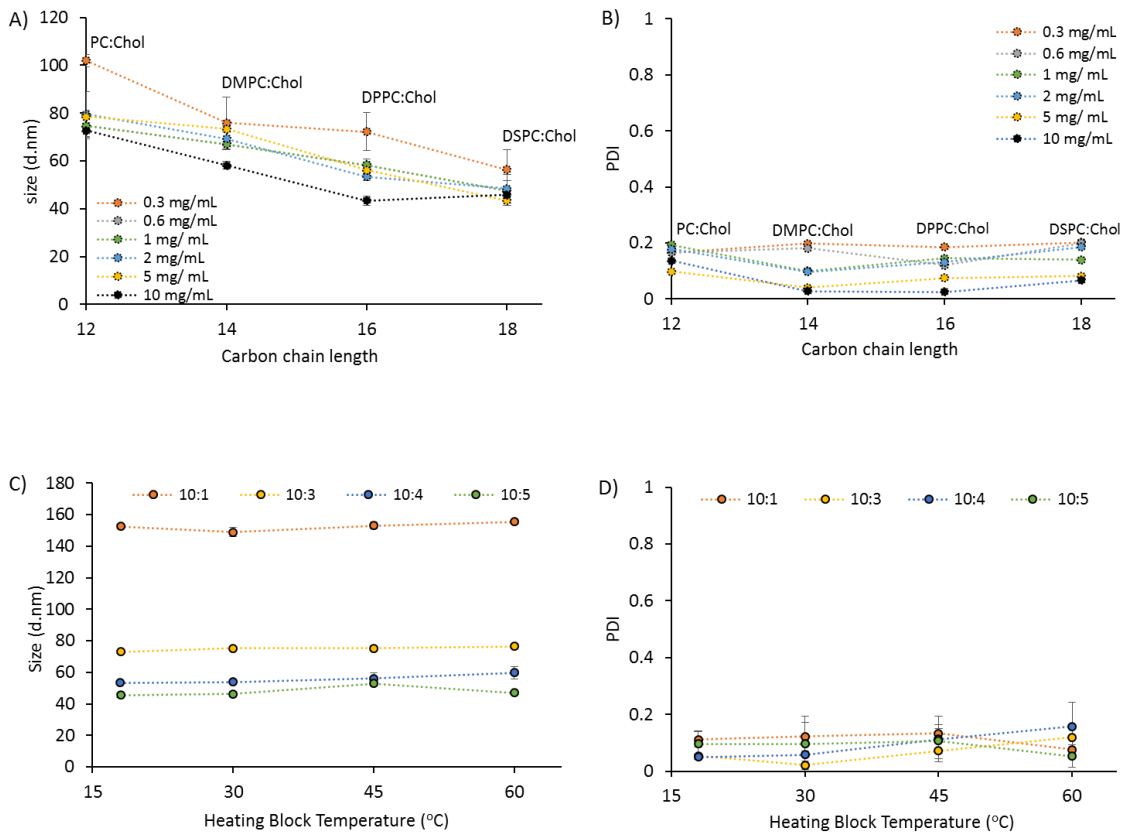
710 **Table 4. Comparison of entrapment of different proteins.** In total three different proteins (Insulin,  
 711 Bovine Serum Albumin (BSA) and OVA) were incorporated into DSPC:Chol liposomes ( 2:1 wt/wt)  
 712 manufactured using microfluidics at a flow rate ratio of 3:1, 15 mL/min TFR and purified via TFF. An  
 713 initial protein concentration of 250  $\mu$ g/mL was employed. Results represent mean  $\pm$  SD, n=3  
 714 independent batches.

Protein	Protein Loading (% of initial amount added)	Liposome Size (d.nm)	Liposome PDI
<b>Insulin (5.7 KDa)</b>	36.8 $\pm$ 2.7	57 $\pm$ 2.9	0.087 $\pm$ 0.062
<b>OVA (42.7 KDa)</b>	34.2 $\pm$ 4.9	53 $\pm$ 2.5	0.219 $\pm$ 0.011
<b>BSA (65.5 KDa)</b>	25.2 $\pm$ 2.8	65 $\pm$ 2.8	0.144 $\pm$ 0.021

715

716

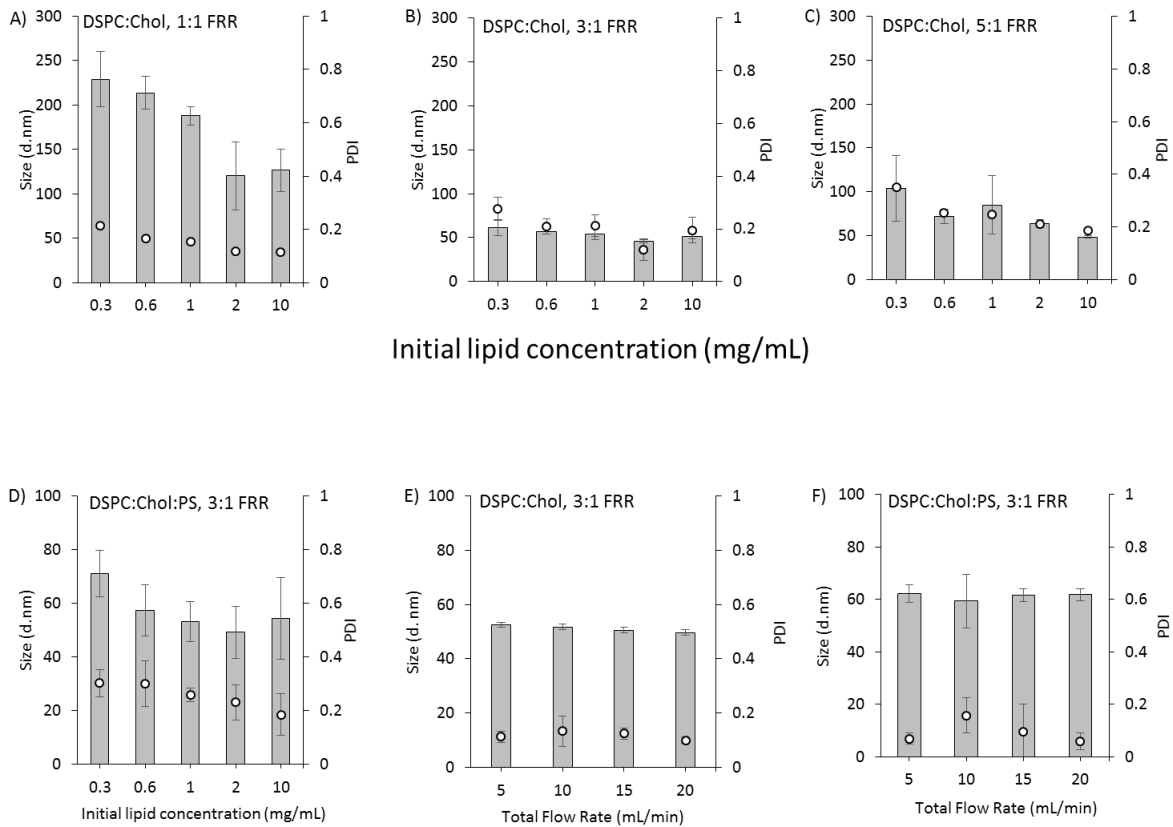
717 **Figures.**



718

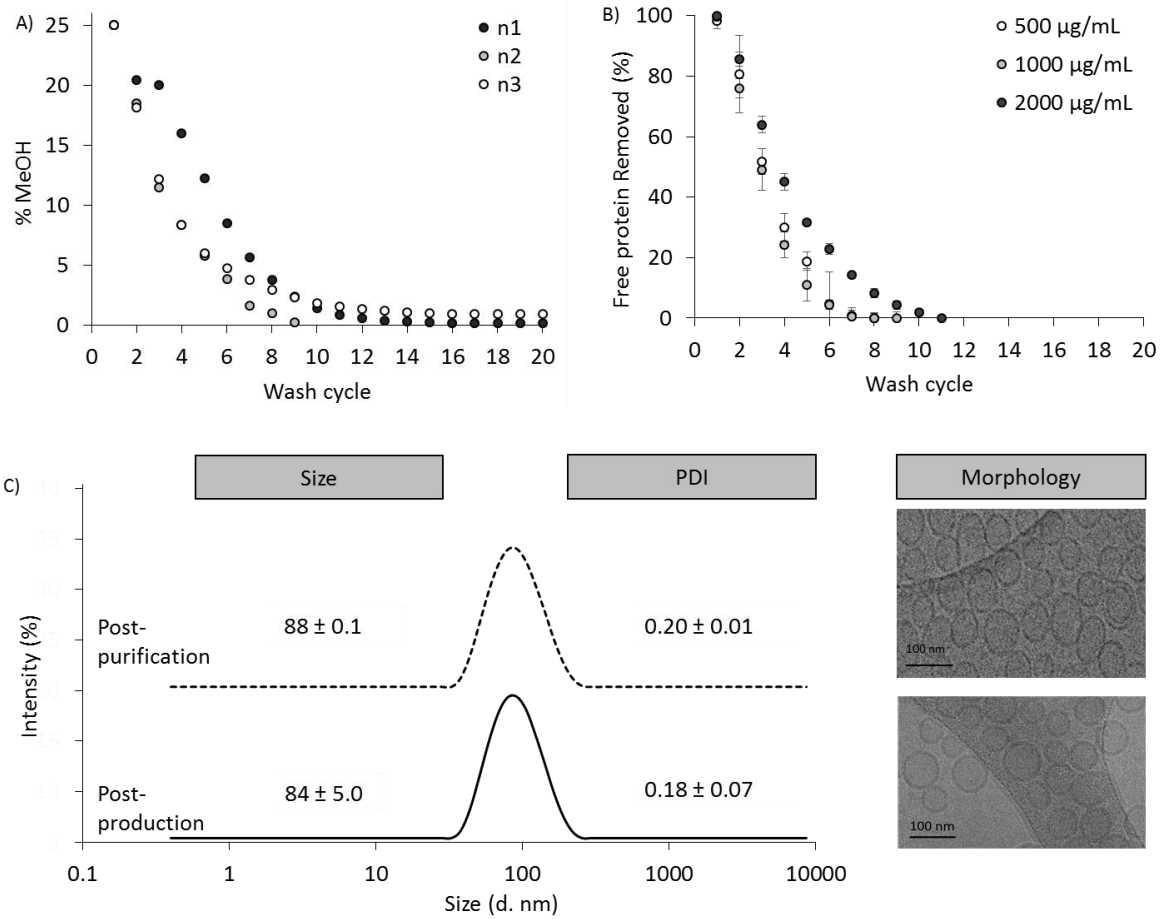
719 Figure 1: The effect of liposomal formulation on physicochemical characteristics of liposomes  
 720 produced by microfluidics. Four liposome formulations (PC:Chol, DMPC:Chol, DPPC:Chol, and  
 721 DSPC:Chol) with increasing hydrocarbon tail length were manufactured using microfluidics at a 3:1  
 722 FRR, 15 mL/min TFR and purified using dialysis. The effect of PC lipid chain length on A) liposomes z-  
 723 average size (d.nm) and B) PDI. DSPC:Chol liposomes were selected and the effect of cholesterol  
 724 content and heating block temperature were investigated in regards to C) z-average particle size and  
 725 D) PDI. Results represent mean  $\pm$  SD, n=3 independent batches.

726



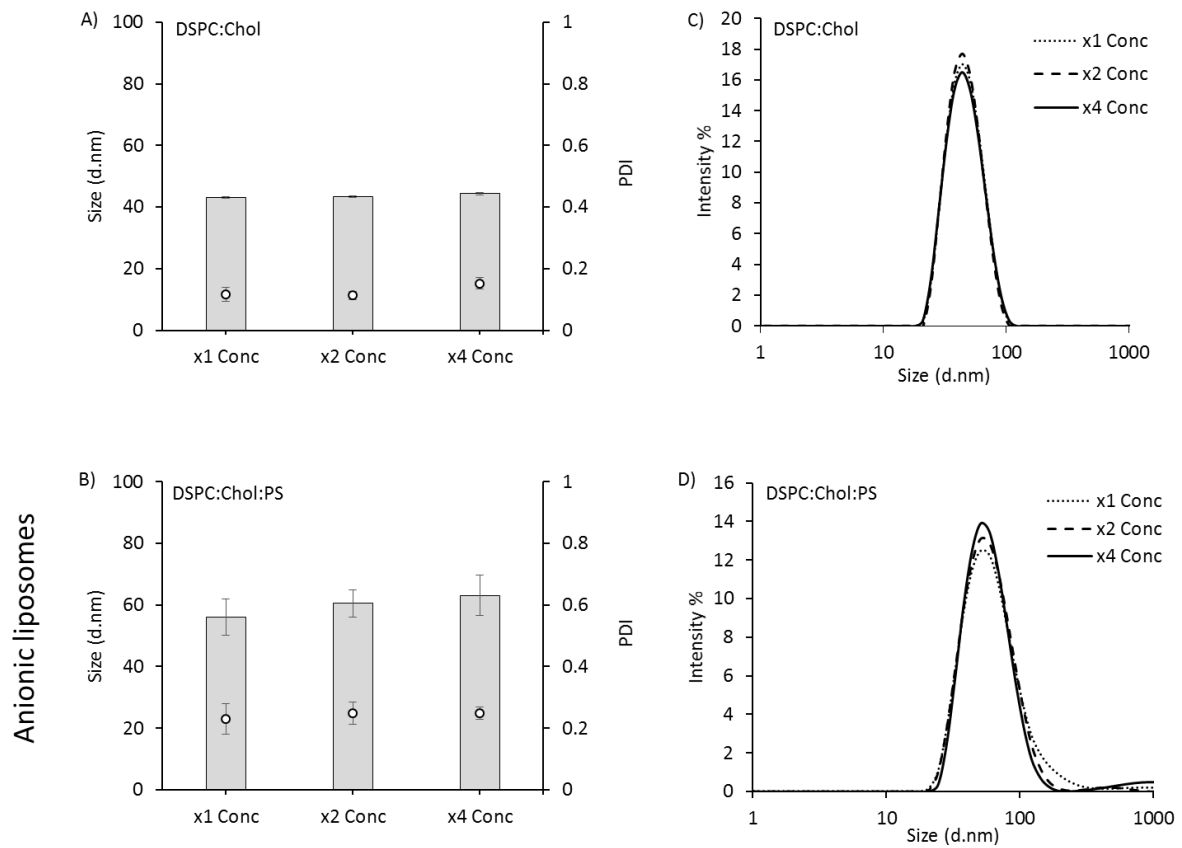
727  
 728 Figure 2: The effect of microfluidic parameters on neutral and anionic liposome attributes. The effect  
 729 of the initial lipid concentration on average liposome size (d.nm; represented by bars) and PDI  
 730 (represented by discrete points) for liposomal formulation DSPC:Chol (10:5 wt/wt) (10 mL/min TFR)  
 731 at a flow rate ratio of A) 1:1, B) 3:1, and C) 5:1. D) The effect of increasing initial lipid concentration on  
 732 z-average particle size (d.nm) for DSPC:Chol:PS (10:5:4 wt/wt) (3:1 FRR, 10 mL/min TFR). E)  
 733 Investigating the effect total flow rate (mL/min) on z-average particle size (d.nm) and PDI for liposomal  
 734 formulation DSPC:Chol (4 mg/mL initial lipid, 3:1 FRR). F) The effect of total flow rate (mL/min) for  
 735 anionic formulation DSPC:Chol:PS (4 mg/mL initial lipid, 3:1 FRR). Results represent mean  $\pm$  SD, n = 3  
 736 of independent batches.

737



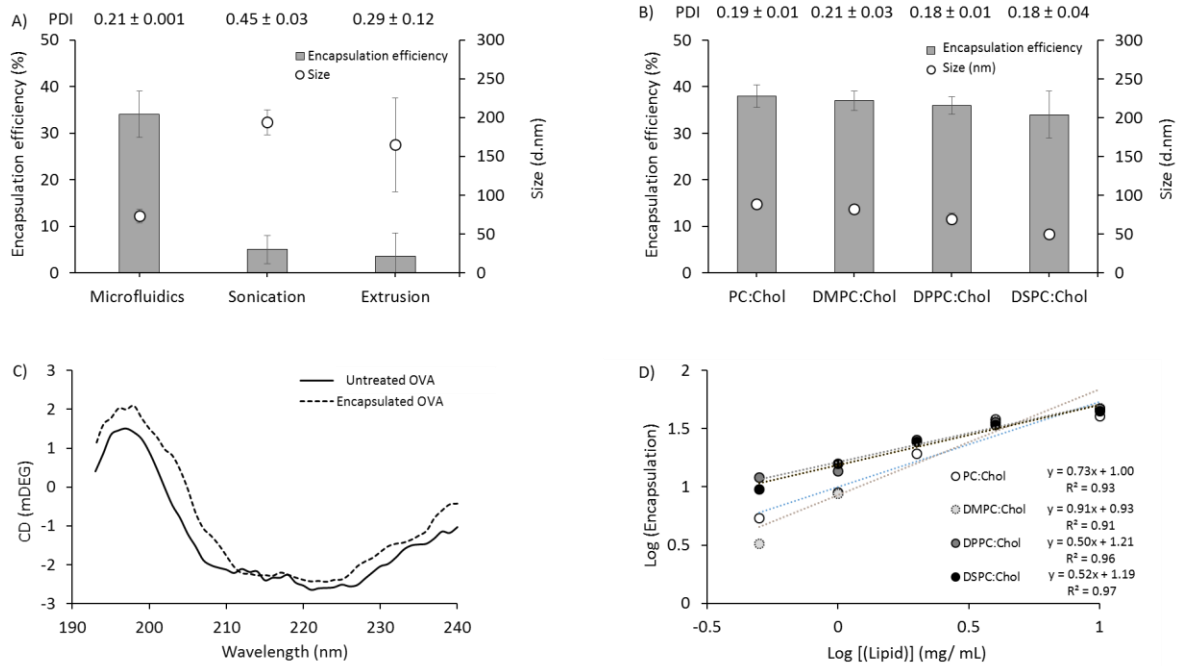
738  
 739 Figure 3: Purification of liposomes using tangential flow filtration (TFF). Liposomes (DPPC:Chol; FRR  
 740 3:1, 15 mL/min TFR) were prepared and characterised as follows: A) Residual solvent (methanol)  
 741 remaining in liposomes after consecutive wash cycles, B) removal of non-incorporated protein via TFF,  
 742 C) liposome attributes before and after purification via TFF and cryo-EM images of liposomes before  
 743 and after TFF purification. Results represent mean ± SD, n =3 of independent batches.

744



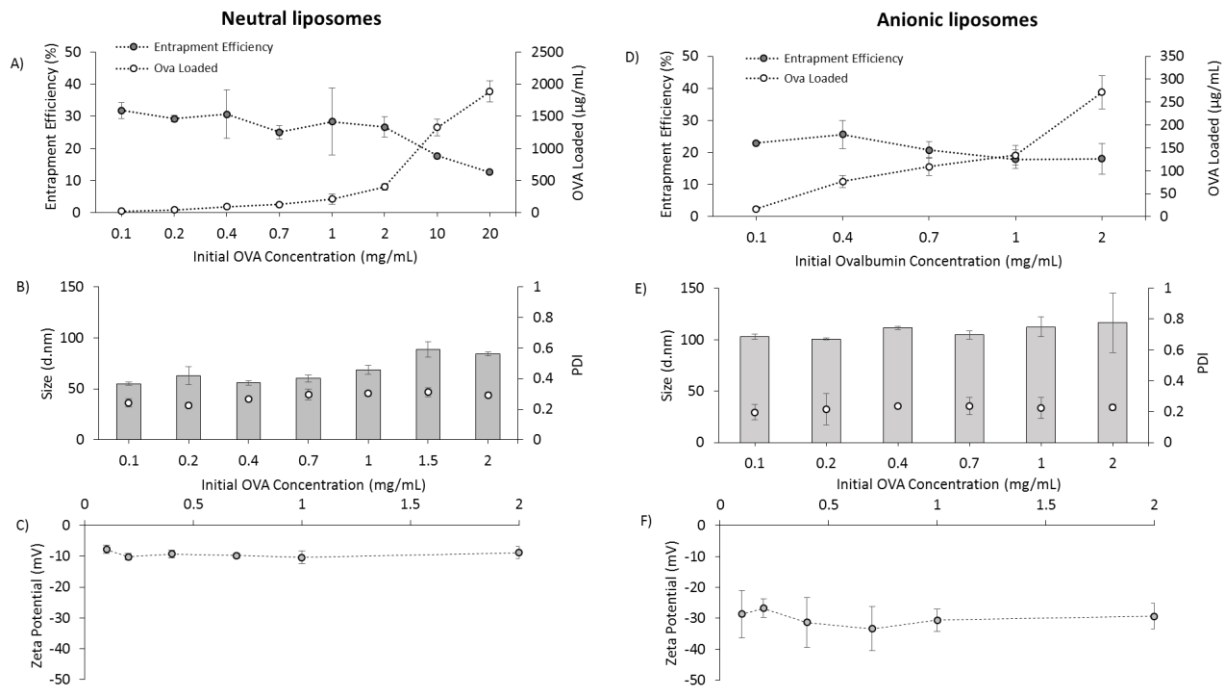
745  
 746 Figure 4: Concentration of liposomal formulations using tangential flow filtration. DSPC:Chol (10:5  
 747 wt/wt) and DSPC:Chol:PS (10:5:4 wt/wt) were prepared at 4 mg/mL initial lipid concentration, 3:1  
 748 FRR, 15 mL/min TFR following microfluidics, followed by 1,2 and 4 fold concentration steps. Particle  
 749 Size (Z-Avg; represented by bars) and PDI (represented by discrete points) for A) DSPC:Chol and B)  
 750 DSPC:Chol:PS both prepared C) and D) are intensity plots for the same conditions. Results represent  
 751 mean  $\pm$  SD, n =3 of independent batches.

752



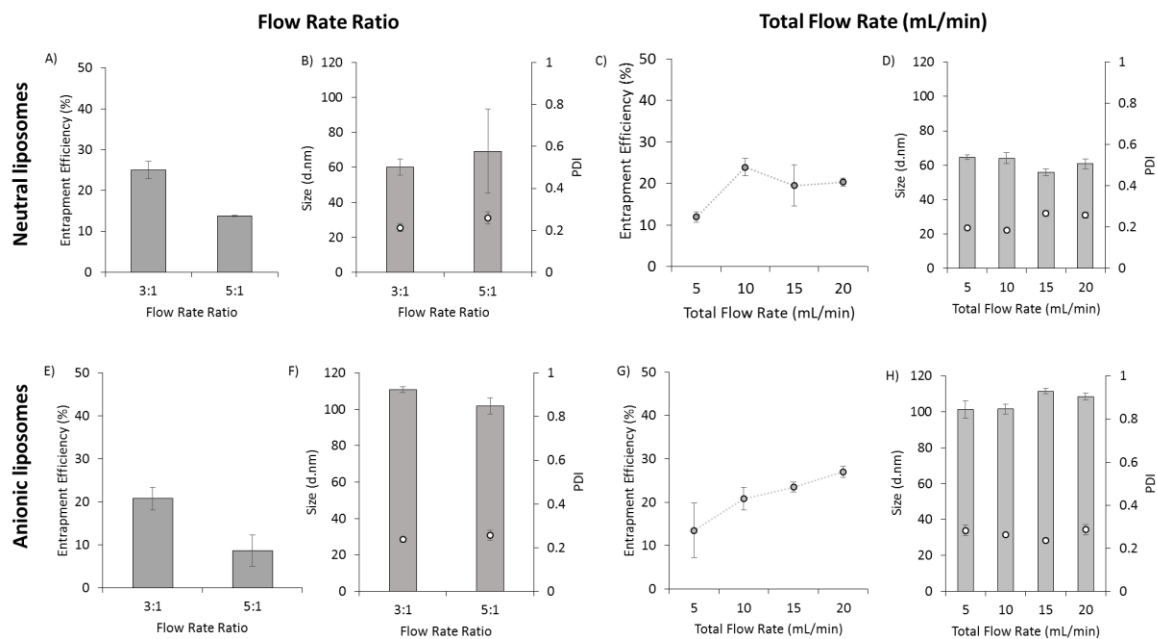
753  
754  
755  
756  
757  
758  
759  
760  
761  
762  
763  
764  
765  
766

Figure 5. Manufacture of protein loaded liposomes using microfluidics. A) Ovalbumin loading and physicochemical comparison between microfluidics and lipid-film hydration followed by extrusion or sonication. DSPC:Chol (10:5 wt/wt) liposomes were made with 1 mg/mL final total lipid and 0.18 mg/mL ovalbumin. The encapsulation efficiency, size and PDI of the liposomes. B) Microfluidics was further tested with respect to changes in lipid hydrocarbon tail length and concentration. Protein encapsulation, size and PDI for PC:Chol, DMPC:Chol, DPPC:Chol and DSPC:Chol (4 mg/ mL initial lipid and 0.25 mg/ mL Ovalbumin) made using microfluidics (3:1 FRR and 15 mL/ min TFR). C) The structural integrity of ovalbumin loaded into the liposomes measured by circular dichroism. DSPC:Chol (10:5 wt/wt) liposomes were prepared with OVA (8 mg/mL initial total lipid and OVA, 3:1 FRR, 15 mL/min TFR) and purified via TFF. Spectra was measured across 180 – 260 nm D) Log-log plot of lipid concentrations (0.5- 10 mg/ mL) against encapsulation efficiency (0.25 mg/ mL ovalbumin). Results represent mean ± SD, n=3 independent batches.



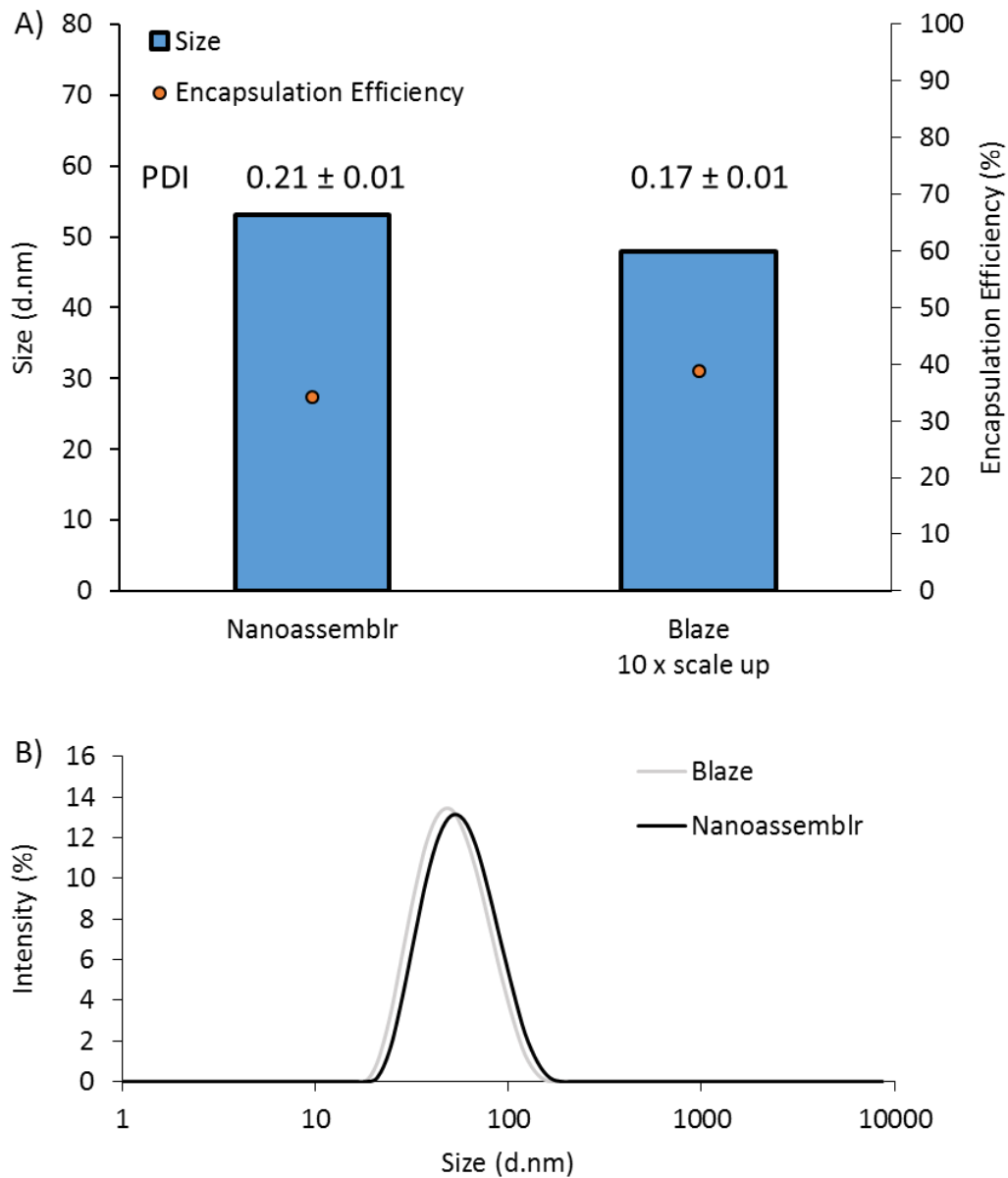
767  
 768 Figure 6: The effect of protein concentration in aqueous phase on entrapment efficiency and liposomal  
 769 physicochemical characteristics for a neutral liposomal formulation (DSPC:Chol; 10:5 wt/wt) (A to C)  
 770 and anionic formulation (DSPC:Chol:PS; 10:5:4 wt/wt) (D to F) using initial total lipid concentration of  
 771 4 mg/mL, 3:1 flow rate ratio and 15 mL/min TFR. A) Entrapment efficiency and protein loading across  
 772 initial ovalbumin concentrations for neutral liposomal formulation. B) Average particle size and PDI,  
 773 and C) Zeta potential for the same formulation. D) Entrapment efficiency and protein loading across  
 774 initial ovalbumin concentrations for anionic liposomal formulation, E) Average particle size and PDI  
 775 and, F) Zeta potential for the same formulation. In B) and E) particle size is shown by bars and PDI is  
 776 shown by discrete points. Results represent mean  $\pm$  SD, n=3 of independent batches.

777



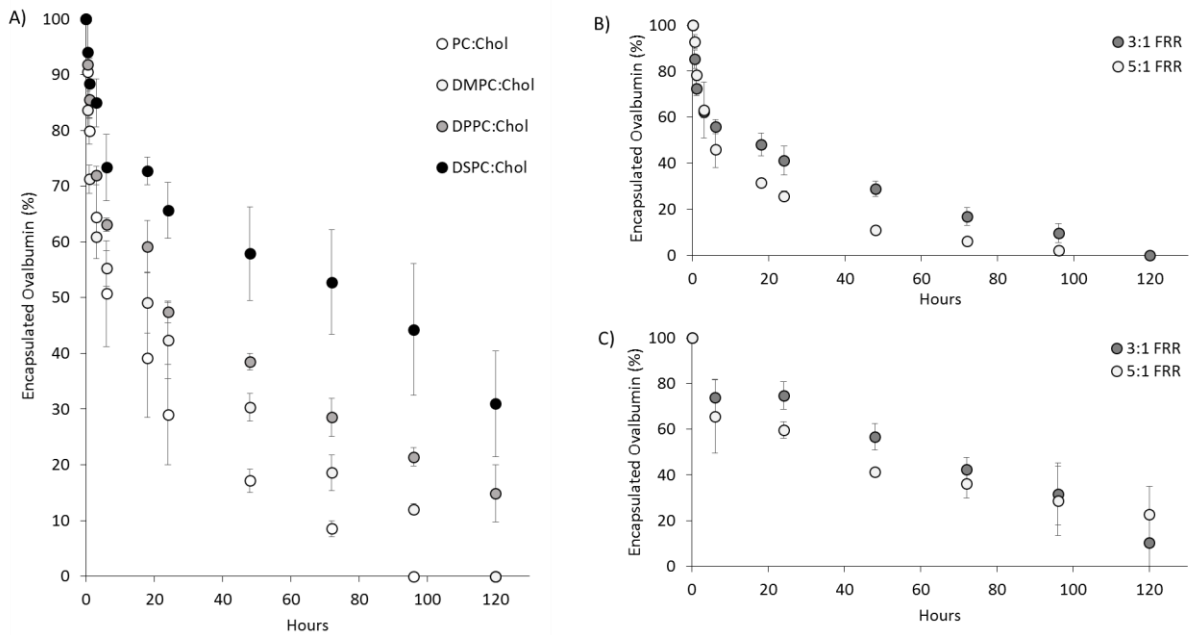
778  
 779 Figure 7: Microfluidic manufacture of neutral and anionic liposomes encapsulating protein. Both  
 780 neutral (DSPC:Chol; 10:5 wt/wt) (A to D) and anionic (DSPC:Chol:PS; 10:5:4 wt/wt) (E to H) were tested:  
 781 A) Entrapment efficiencies for flow rate ratios 3:1 and 5:1 for DSPC:Chol (final lipid and OVA  
 782 concentrations matched at 1 mg/mL and 0.525 mg/mL respectively). B) Average particle size and PDI  
 783 for the same formulation C) Entrapment efficiencies with varying on total flow rate (mL/min) (3:1 flow  
 784 rate ratio, 4 mg/mL and 0.7 mg/mL initial total lipid and OVA respectively) and D) the resulting particle  
 785 size (d.nm) and PDI with varying total flow rate. E) Effect of flow rate ratio on entrapment efficiency  
 786 for DSPC:Chol:PS (final lipid and OVA concentrations matched at 1 mg/mL and 0.525 mg/mL  
 787 respectively). F) Entrapment efficiencies with varying on total flow rate (mL/min) (3:1 flow rate ratio,  
 788 4 mg/mL and 0.7 mg/mL initial total lipid and OVA respectively) and H) the resulting particle size (d.nm)  
 789 and PDI with varying total flow rate. Where appropriate liposome size is shown by bars and PDI is  
 790 shown by discrete points. Results represent mean  $\pm$  SD, n=3 of independent batches.

791



792 Figure 8: Proof-of-concept scale-out studies. DSPC:Chol liposomes were prepared at a FFR 3:1, TFR 15  
 793 mL/min, and a concentration of 10 mg/mL on both the NanoAssemblr (total volume 2 mL) and Blaze  
 794 (total volume 20 mL). A) The protein loading, size and polydispersity index (PDI) of both batches and  
 795 B) an overlay of the intensity plots for both batches.

797



798

799

800

801

802

803

804

805

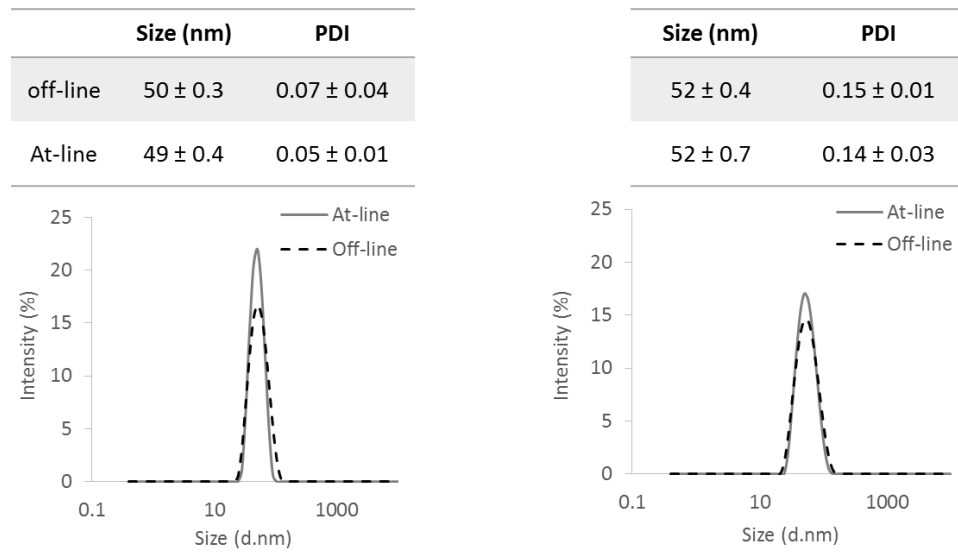
806

807

Figure 9. Protein release from liposome formulations manufactured by microfluidics. A) The release of OVA from PC:Chol, DMPC:Chol, DPPC:Chol and DSPC:Chol liposomes produced at a 3:1 ratio (15 mL/min TFR) over 120 hours. B) Ovalbumin release from DMPC:Chol liposomes produced at a 3:1 and 5:1 FRR (15 mL/min TFR.) C) Ovalbumin release from DSPC:Chol liposomes produced at a 3:1 and 5:1 FRR (15 mL/min TFR, matched at a final concentration of 1 mg/mL total lipid, 0.1875 mg/mL OVA) Liposome suspensions were kept at 37°C with agitation. At set times, the sample was collected the OVA remaining inside the liposomes quantified. The results represent the mean of three independent batches  $\pm$  SD.

807

Production      In-process monitoring      Purification      Product validation



808

809

810

811

812

813

814

815

816

817

818

Figure 10: Liposome at-line particle size monitoring as part of a production train. DSPC:Chol liposomes were prepared at a FFR 3:1, TFR 15 mL/min, and a concentration of 10 mg/mL. The size and polydispersity index (PDI) of all formulations were measured (at a ratio of 1:10) off-line using the Zetasizer Nano ZS (Malvern Instruments, Malvern, UK) or at-line as part of the automated continuous manufacturing process using the Zetasizer AT (Malvern Instruments, Malvern, UK). To characterise liposomes in real time, the Zetasizer AT measured liposome size and PDI at a 1:10 dilution (liposomes to buffer), with adjustments to the automated mixing possible. The buffer (5 mL/min) and liposome formulation (0.5 mL/min) are taken up by the instrument, and enter into the flow cell where the size and PDI was measured. A total of 1 mL was required for each size measurement. Liposome formulations were purified using the KrosFlo Research Iii TFF system.